WRC RESEARCH REPORT NO. 110

E X P E R I M E N T A L S T U D I E S O F W I N G - W A L L M I X I N G C O N T R O L

by

W. Hall C. Maxwell
Associate Professor of Civil Engineering
and
Misganaw Demissie
Research Assistant in Civil Engineering

University of Illinois at Urbana-Champaign

F I N A L R E P O R T

Project No. B-083-ILL

July 1, 1973 - December 31, 1975

This project was partially supported by the U.S. Department of the Interior in accordance with the Water Resources Research Act of 1964, P.L. 88-379, Agreement No. 14-31-0001-4079.

UNIVERSITY OF ILLINOIS
WATER RESOURCES CENTER
2535 C. E. Hydrosystems Lab.
Urbana, Illinois 61801

February 1976

ABSTRACT

EXPERIMENTAL STUDIES OF WING-WALL MIXING CONTROL

Detailed velocity traverses are presented for shallow submerged slot jets without lateral confinement. With wing-walls in place maximum velocities and temperatures were traced for both unheated and heated discharges. These tests were repeated for various wing-wall crest elevations and wing-wall lengths. For the wing-wall tests a typical Reynolds number based on slot width was 400,000 and a typical densimetric Froude number based on slot width was 40. Some flow combinations were found to be unstable and tests were conducted to delineate the limits of stability. The tests demonstrate that flow patterns may be controlled using controlled flow over wing-wall crests. A simple design procedure making use of the data is illustrated.

Maxwell, W. Hall C., and Demissie, M.
EXPERIMENTAL STUDIES OF WING-WALL MIXING CONTROL
Completion Report to Office of Water Research and Technology, Department of the Interior, Washington, D.C., February 1976, 71 pp.
KEYWORDS - *control structures/ *diffusion/ discharge (water)/ heated water/ *mixing/ outlets/ *outlet works/ pollution abatement/ *thermal pollution/ *waste dilution

CONTENTS

LIST OF FIGURES

LIST OF TABLES

NOTATION

The following symbols are used in this report:

b = height of slot outlet

C = spreading coefficient for momentum flux

D = diameter of circular outlet

F = Froude number, $u_o/\sqrt{gw}$

F_Δ = densimetric Froude number, $u_o/(gw\Delta\rho/\rho)^{0.5}$

g = acceleration of gravity

L = length of wing-wall in downstream direction

T_c = temperature of cold water at mixing valves

T_H = temperature of hot water at mixing valves

T_o = temperature of discharge at slot outlet

T_r = temperature of reservoir outside wing-walls

u = time average velocity in x-direction

u_m = maximum value of u for fixed x

u_o = value of u at outlet (assumed uniform)

w = width of slot outlet

x = coordinate in direction of jet axis, positive downstream

x_o = zero correction or origin shift for x

x_s = value of x at which maximum velocity reaches free surface

y = lateral coordinate measured from slot centerline

z = vertical coordinate measured from free surface

z_m = value of z at which $u = u_m$

z_o = submergence of slot outlet centerline below free surface

z_t = distance from centerline of slot to top of wing-wall, measured vertically

$\Delta\rho$ = density of reservoir water minus density of heated discharge

ρ = density of reservoir water

$\Delta T = T_H - T_c$

I. INTRODUCTION

It has been observed, in laboratory investigations by Mross (7)* and by Maxwell and Pazwash (4,5) that a shallow submerged axisymmetric jet deflects towards the free surface downstream from the outlet. The behavior is illustrated in Fig. 1, which has been calculated from the theoretical model developed by Maxwell and Pazwash (6) for a horizontal nozzle at a submergence of five diameters. Figure 1 shows vertical axial velocity profiles downstream from the outlet. Initially the velocity profiles do not differ radically from those for an infinitely submerged jet. However, with increasing distance downstream the velocities above the nozzle axis increase relative to those below the axis. As a consequence, the maximum velocity moves above the original nozzle axis and migrates upward with increasing distance downstream, eventually reaching the free surface. It will be observed from Fig. 1 that, as the maximum velocity approaches the free surface the profiles in the vicinity of the maximum become rather flat making it difficult to experimentally locate the maximum accurately even when there is small scatter in the experimental data.

The mathematical model developed in Ref. 6 was shown to agree well with experimental data for a horizontal outlet and for an outlet with small upward deflection. Figure 2 illustrates the latter case and shows the sensitivity of the flow pattern to a small upward deflection of the outlet axis.

In view of the good agreement between theory and experiment found for the axisymmetric outlet it would be reasonable to expect that a

*Numerals in parentheses refer to corresponding items in List of References.

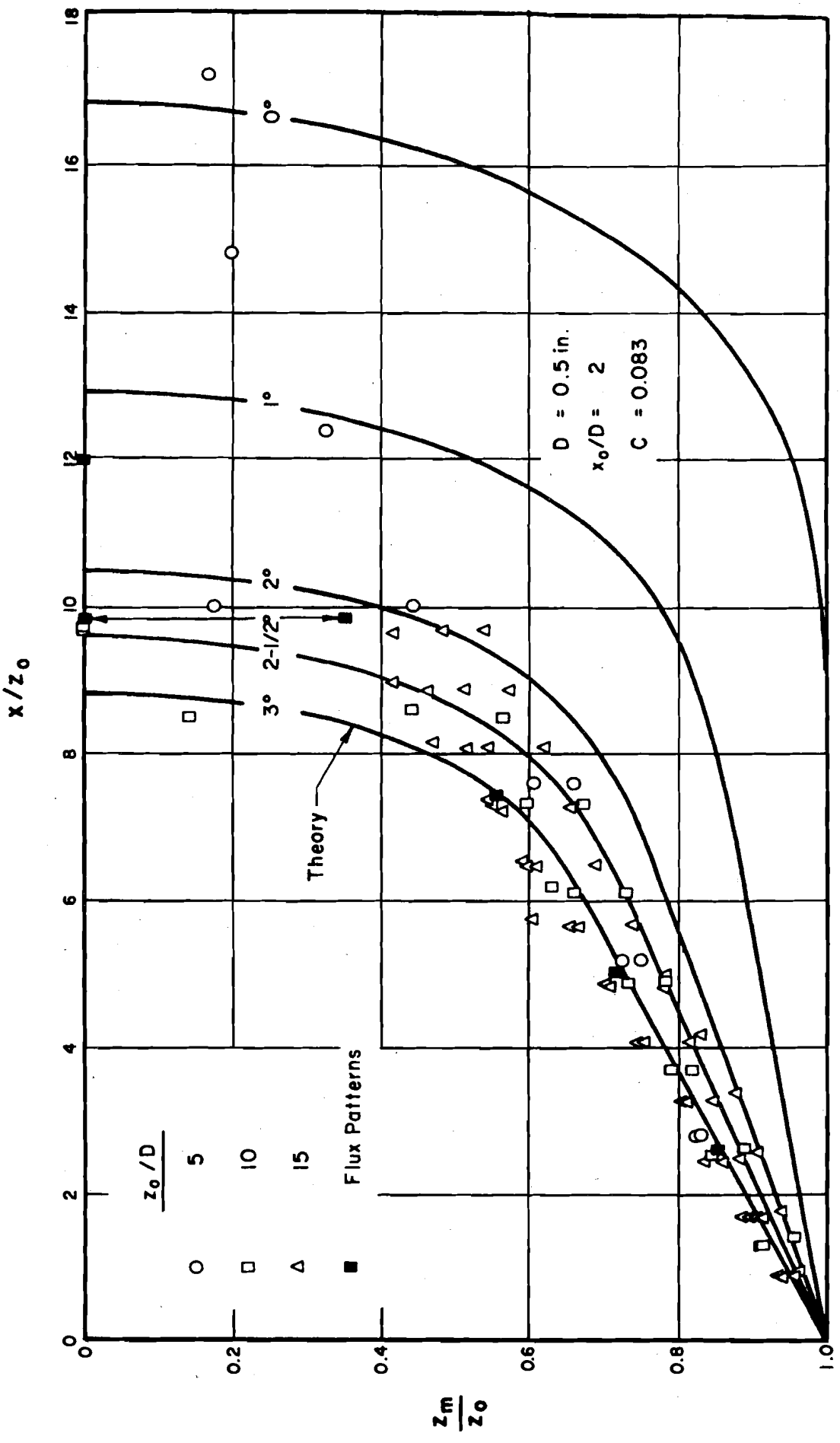

Fig. 2 Vertical centerline location of filament of maximum flux for shallow submerged jet with small initial upward deflection.

plane-symmetric equivalent of the axisymmetric analysis would be useful in predicting the center-line velocity profile downstream from a slot outlet. If the time average value of the square of the turbulent fluctuating component of velocity in the horizontal downstream direction ($\overline{u'^2}$) is treated as negligible the plane symmetric analysis yields the following solution for the location of the maximum velocity downstream from a horizontal plane symmetric outlet (6):

$$\left(\frac{Cx}{z_o}\right)^2 = \frac{2\, z_m/z_o}{\text{arctanh}(z_m/z_o)} \qquad (1)$$

in which C = spreading coefficient for momentum flux; x = co-ordinate in direction of jet axis; z_o = vertical submergence of the outlet center-line below the free surface; and z_m = vertical co-ordinate of the maximum velocity. The location, x_s, at which the maximum flux reaches the free surface is given by

$$x_s/z_o = \sqrt{2}/C \qquad (2)$$

Figure 3 shows a comparison between Eq. 1 and the experimental measurements downstream from a 1/8-in. (0.32 cm) by 6-in. (15.24 cm) slot in a 6-in. (15.24 cm) wide channel by John, Mahajan and Kanbour (2,3). Equation 1 was evaluated using C = 0.109, the value obtained by Albertson et al (1) for wide plane symmetric outlets of various aspect ratios. Thus, Eq. 2 indicates that the maximum velocity should reach the free surface at 13.0 diameters downstream from the outlet. Figure 3 shows that the analysis is in radical disagreement with the data of John et al. The explanation, however, is that the presence of the lateral sidewalls of the channel used by John et al cut off entrainment to the upper side of the jet and trap a vortex in the zone bounded by the back wall, the

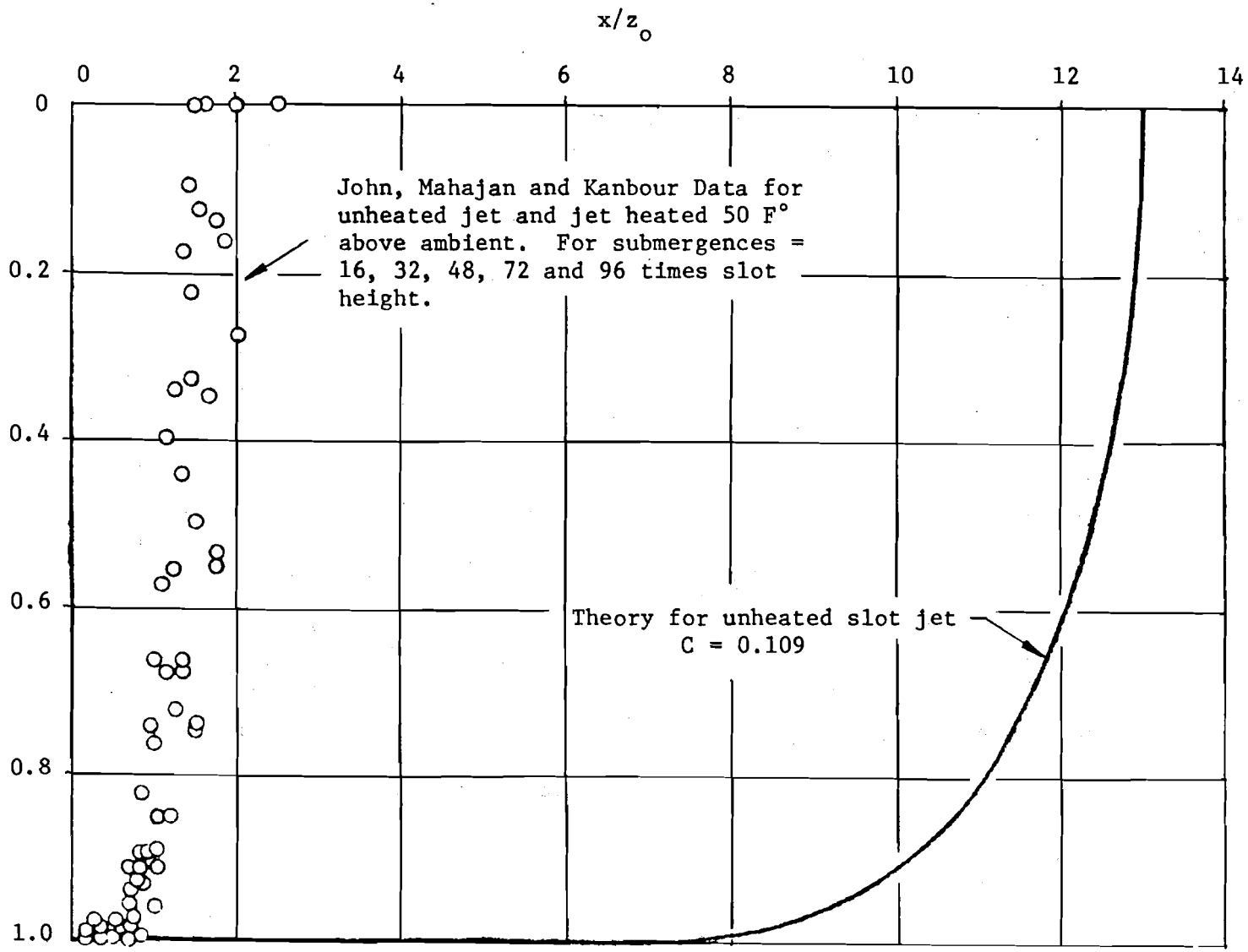

Fig. 3 Vertical centerline location of filament of maximum flux for shallow submerged horizontal slot jet.

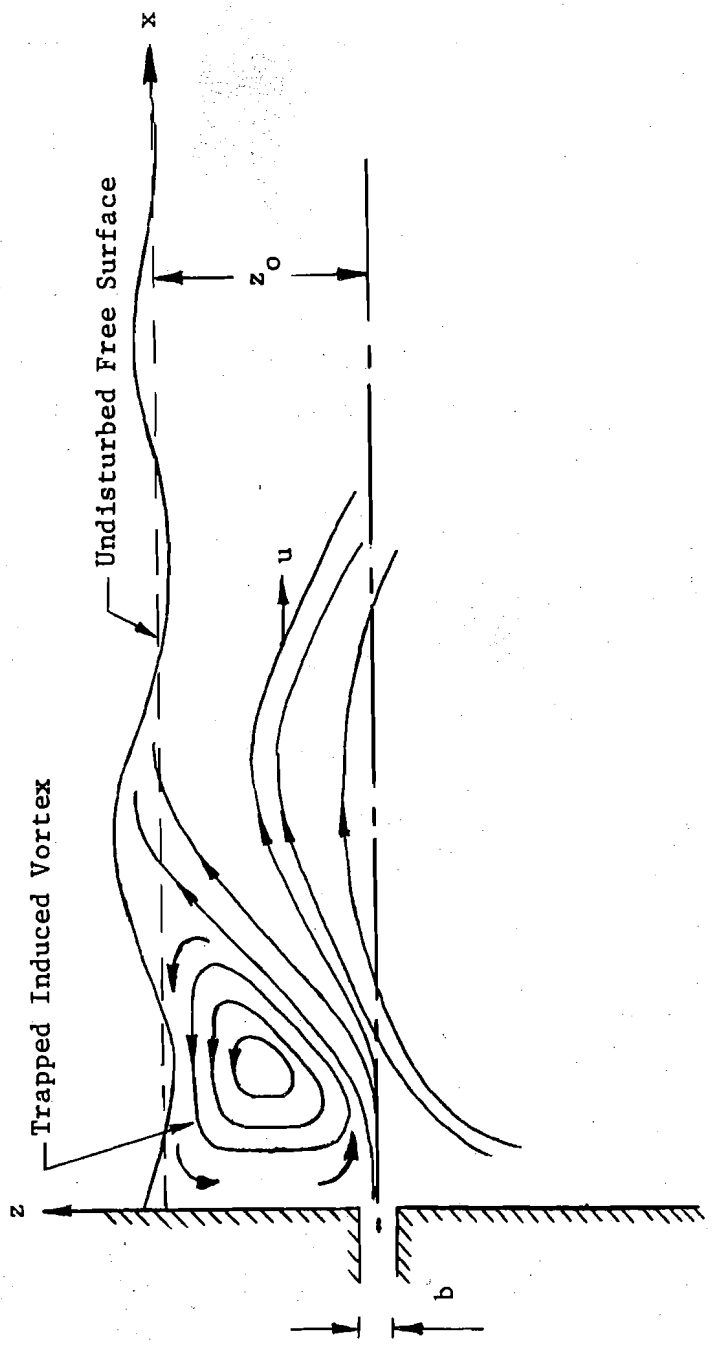

Fig. 4 Schematic representation of flow pattern for submerged slot outlet showing vortex trapped by confining sidewalls.

sidewalls and the upper edge of the discharge jet (Fig. 4). That this vortex and its effect dominates the flow pattern is indicated by the fact that John et al found no difference in behavior between cold water discharges and discharges heated $50F^{o}$ above ambient, until the submergence of the outlet was increased to 120 times the slot height. An analysis of this behavior was presented by Stoy, Stenhouse and Hsia (8). Stoy et al reproduced the experiments of John et al and found good agreement except for the maximum submergence of 120 slot heights.

Presuming for the moment that the theoretical analysis presented in Fig. 3 is valid when there is no cut-off of entrainment to the region above the jet, Fig. 3 indicates the possibility of controlling the flow pattern and mixing downstream from a slot outlet by controlling the discharge to the bounded region above the outlet, either through openings in the lateral sidewalls or over the top of the sidewalls. By having variable gates in either location and adjusting their openings the flow pattern could be controlled over a wide range. This could prove useful in meeting regulations governing temperature conditions in the vicinity of discharge outlets for power plant cooling water discharges. With the minimum entrainment denoted by the experiments of John et al temperatures would remain high in the outlet vicinity leading to more rapid transfer of heat to the atmosphere. Should this result in temperatures in excess of those permitted by regulation a controlled inflow to the region above the outlet could be used to bring the maximum temperature within limits while keeping the heated zone as small as possible and thereby transferring heat to the atmosphere as rapidly as possible.

II. APPARATUS AND EXPERIMENTAL PROCEDURE

The experimental apparatus is shown schematically in Fig. 5. Either cold or heated water was supplied to a head chamber constructed using a 4-ft (1.22 m) long spool of 8-in. (20.3 cm) diameter cast iron pipe, part of which was packed with rubberized hair to straighten the flow. The chamber was supplied with cold water from the laboratory constant head tank which has a crest elevation approximately 53-ft (≈16 m) above the main laboratory floor. When supplying heated water (or cold water through the heater assembly) the head tank was assisted by a Goman Rupp 81 1/2 B2 E1 1/2 self priming centrifugal pump which has a fairly steep head-discharge characteristic. The water was heated using two Duro-Power 40.5 KW heaters. The heating system is capable of delivering 2460 GPH (9312 liters per hour) of water at a temperature of 20F^{o} (12.2 C^{o}) above ambient. The discharge is accurately controlled using automatic precision mixing valves. The inlet nozzle had its outlet flush with the back wall of the tank and maintained constant dimensions of 6-in. (15.24 cm) ± 0.001 in. wide by 1/8-in. (3.175 mm) ± 0.002 in. back for a distance of 7 11/16-in. (19.52 cm) before expanding, using a 3 to 1 elliptical transition both horizontally and vertically over the next 1 5/16-in. (3.33 cm), to 6 7/8-in. (17.46 cm) wide by 1 in. (2.54 cm) high at the entrance chamber.

The test tank was 16-ft (4.88 m) long by 4-ft (1.22 m) wide and 4-ft (1.22 m) deep. The discharge outlet was set at the center of the back-wall 2 1/2-ft (76 cm) above the floor. For heated water tests a cold water diffuser was inserted in the tank as illustrated in Fig. 5. The diffuser was set at the same elevation as the discharge slot. The water elevation in the test reservoir was controlled using a variable tailgate at the downstream end of the tank.

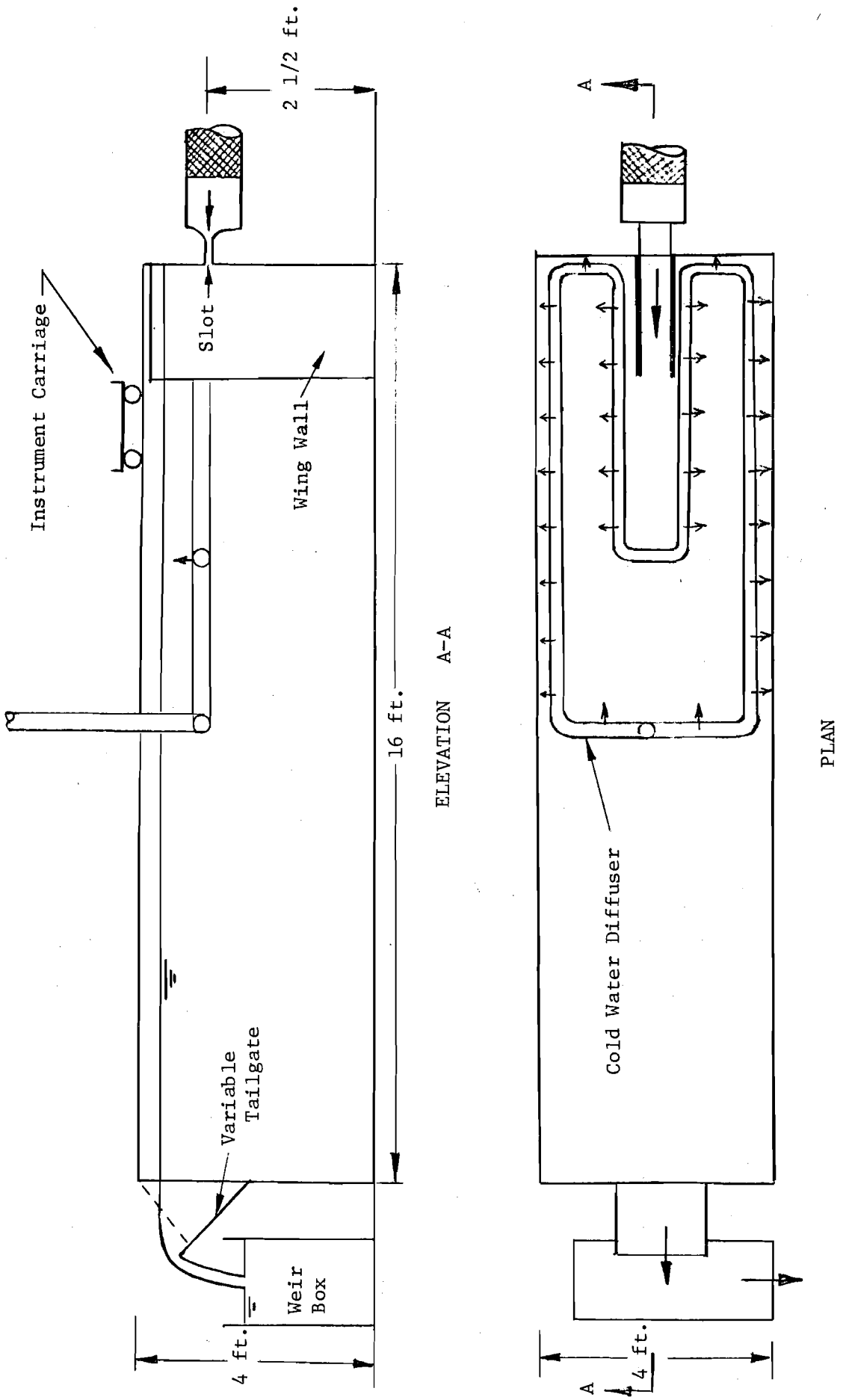

Fig. 5 Schematic representation of experimental apparatus

The water dropped into a 10^{o} V-notch weir tank for measurement of discharge. An instrument carriage ran on rails mounted on the reservoir sidewalls and had a platform which ran on carriage cross-rails. A separate personnel carriage ran on floor rails. The wing-walls were constructed of 3/4-in. (1.9 cm) plywood and extended from the floor of the reservoir upward. They were attached to the sidewalls of the reservoir with braces to maintain a constant spacing of 6 1/4-in. (15.88 cm) and initially extended 2-ft (61 cm) downstream. They were reduced in length for some later experiments. Wooden surfaces were thoroughly sealed using several coats of epoxy resin. The elevation of the top of the wing-walls relative to the free surface for a given submergence of the slot outlet (established using the variable tailgate) was varied using sheets of 1/8-in. (0.3175 cm) plexiglass clamped to the inside of the wooden wing-walls. The net spacing between the plexiglass plates was therefore 6-in. (15.24 cm) and was the same as the slot width. The plexiglass plates extended well below the elevation of the slot outlet and their horizontal top edge could be set at various elevations relative to the reservoir free surface.

Two different systems were used for measurement of velocity. For velocities ranging from about 1.5-ft/sec (45.7 cm/sec) to about 20-ft/sec (6.1 m/sec) measurements were made using a 5/16-in. (0.79 cm) O.D. pilot tube with 1/8-in. (0.32 cm) port connected across a Hewlett-Packard Model 267 BC differential pressure transducer. The output was recorded on a Sanborn recorder. The transducer-recorder system was calibrated at the beginning of each day's work by reference to a differential manometer under static conditions. For lower velocities (down to 6 cm/sec) a Kent Miniflo Type 265 current meter was used with the output recorded on a Technirite Electronics TR-711 recorder. This system was calibrated in a

specially constructed low velocity circular nozzle calibration tank in the laboratory.

Temperatures were measured using a RET-1 thermocouple probe with a time constant of 3.1 seconds in conjunction with a Bailey Digital Amplifying Thermometer, Model BAT-8.

Temperature and velocity probes were located with reference to the center-line of the slot opening. Probes were mounted on Lory point gages, with vernier readings to 0.001-ft for vertical measurements. Lateral measurements were made on steel tape with 0.01-ft divisions attached to the instrument platform cross-rails after the instrument platform had been clamped in position on the instrument carriage. Longitudinal distances downstream from the slot were read from a steel tape with 0.01-ft divisions on the carriage rails after the carriage had been clamped in position.

For those tests in which the cold water diffuser was needed to prevent heat buildup in the reservoir and for which comparisons were desired with a cold water discharge the following procedure was used. First, cold water was run through the heater assembly and the discharge measured using the weir tank. Then the diffuser was turned on and the sum of the two discharges measured. The cold water experiments were then completed. The heater was turned on and the hot water experiments completed. Next the sum of the hot water and diffuser discharges was measured. Finally, the diffuser was turned off and the hot water discharge measured alone. The slight variation in reservoir elevation was judged to have negligible effect on the discharge. The hot water discharge was generally found to be slightly less than the cold water discharge, possibly due to changes in the internal geometry of the flow system, particularly in the precision mixing valves.

The use of the cold water diffuser did not completely eliminate

heat build-up in the reservoir. Generally, by allowing the hot water discharge to run for 30 to 45 minutes before beginning any measurements the heat build-up over the course of the measurements could be reduced to 1 F^{o} or less. For all experiments the temperature of the laboratory supply fed to the heaters remained essentially constant for the duration of the experiments. The total capacity of the laboratory sump system is approximately 17,000 ft^3 so that it was relatively unaffected by the addition of heated water at a rate of 150 ft^3 per hour. The sump temperature, T_c, was read at the precision mixing valves while the cold water was running, but before the heaters were switched on. After the heaters were switched on and allowed to run for some 30 to 45 minutes the hot water temperature, T_H, at the precision mixing valve outlet was read. It was checked occasionally, particularly at the end of any measurements and not found to vary. Therefore the difference between hot water temperature and the cold water temperature at the mixing valve outlet ($\Delta T = T_H - T_c$) has been used to characterize the experiments. It should be noted that there was heat loss to the atmosphere between the outlet of the precision mixing valves and the discharge slot and that during the initial 30 to 45 minute running period the reservoir temperature rose several degrees above that of the sump. Therefore, the values of T_H and T_c should not be used to calculate densimetric Froude Numbers. The relationship between these temperatures and the conditions at the reservoir will be dealt with in more detail in Section III-6.

III. EXPERIMENTAL RESULTS

III-1. Cold Water Discharges Without Wing-walls

In order to provide a sound basis for future development of an analytic model which will adequately take into account variations in spreading coefficient across the flow section considerable effort was initially expended on the collection of complete velocity traverses using discharge water which was at the same temperature as the reservoir without any wing-walls in place. Both vertical and lateral traverses in the flow section were made and the experimental information collected for three different submergences of the slot outlet at a number of sections at different distances downstream from the outlet. The results are shown in Figures 6 through 28. These plots show isovelocity ratio lines, namely plots of u, the local longitudinal time-averaged velocity divided by u_m, the maximum value of longitudinal time-averaged velocity recorded for the section at intervals of 0.1. The location of the maximum value or values recorded for each section is marked with an "X" on the plot. When the observor is positioned at the slot outlet facing in the downstream, x, direction the positive value of y is to the right of the slot centerline.

It will be observed from an inspection of these plots that the velocity profiles are not perfectly symmetrical about the centerline. The appearance of off-center peaks in the velocity profiles of other slender three-dimensional jets has been noted by other observors (9,10,11). In practically all cases, however, it may be noted that a vertical traverse along the slot centerline ($y/x = 0$) will provide a reasonably accurate measurement of the maximum's vertical location even though the maximum may be located off-center. Because the collection of data in the quantities necessary to generate the plots shown in Figs. 6 through 28 required an excessive investment of time and effort it was decided to characterize

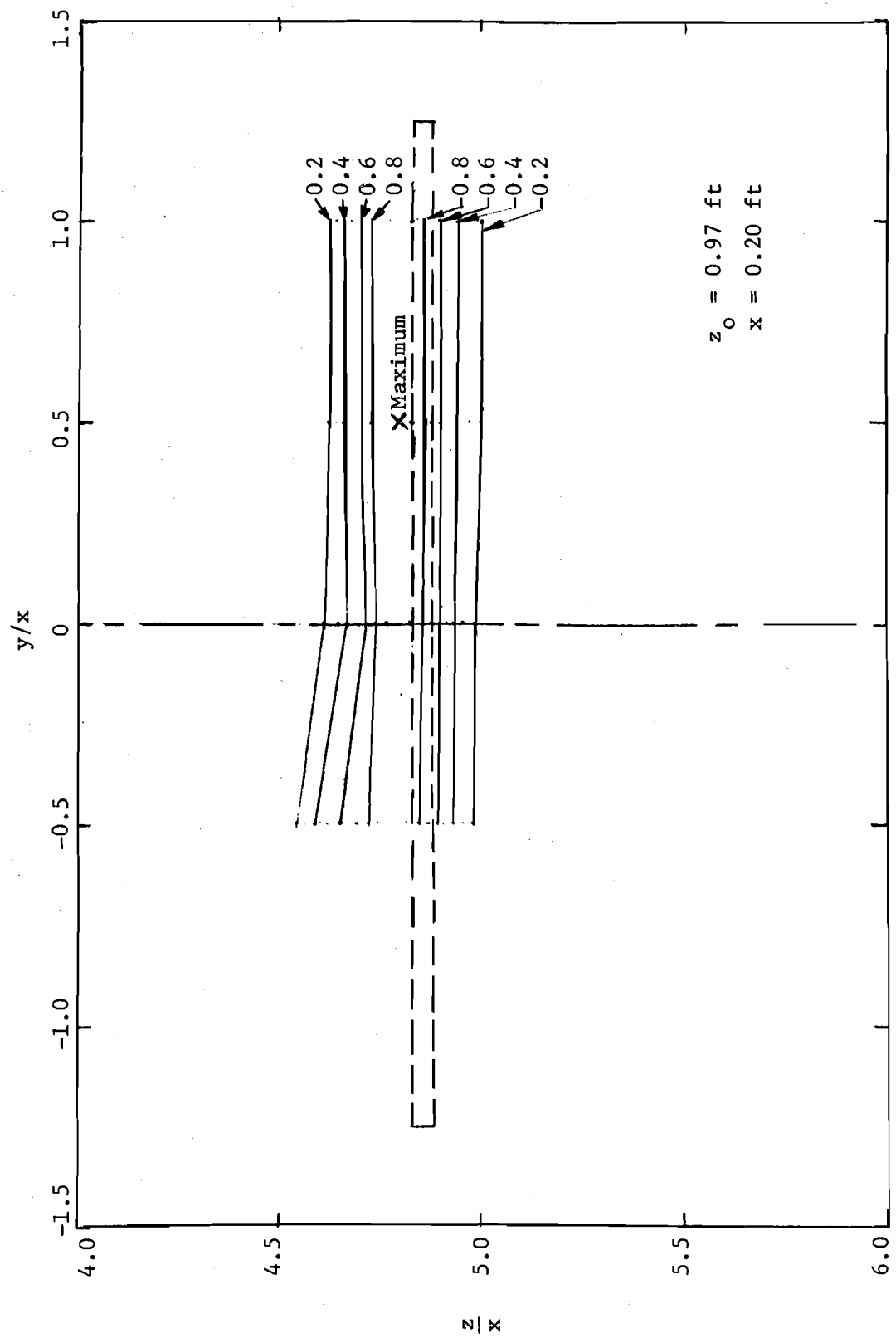

Fig. 6 Isovelocity pattern for unconfined slot discharge submerged 0.97 ft at 0.20 ft downstream from outlet

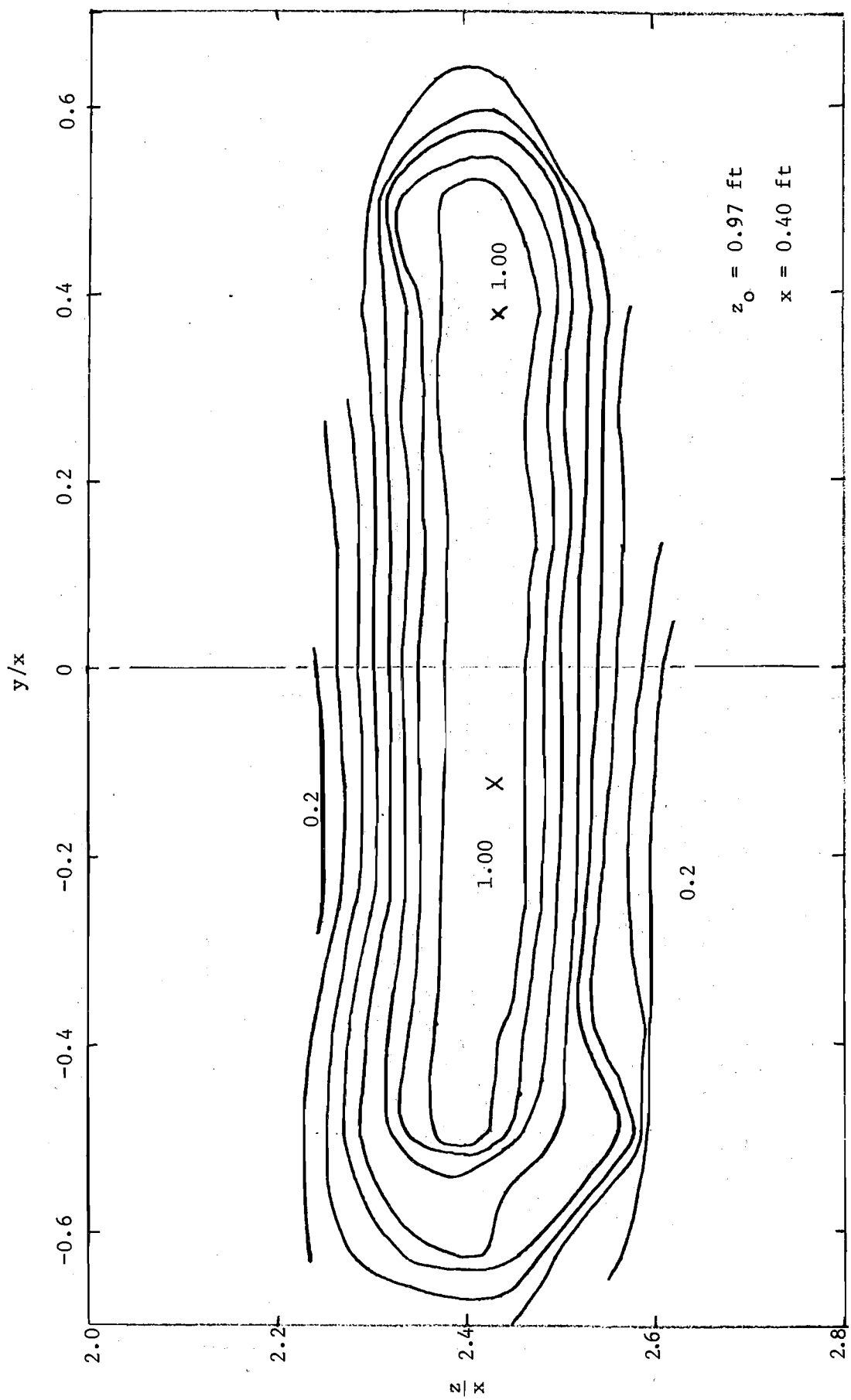

Fig. 7 Isovelocity pattern for unconfined slot discharge submerged 0.97 ft at 0.40 ft downstream from outlet

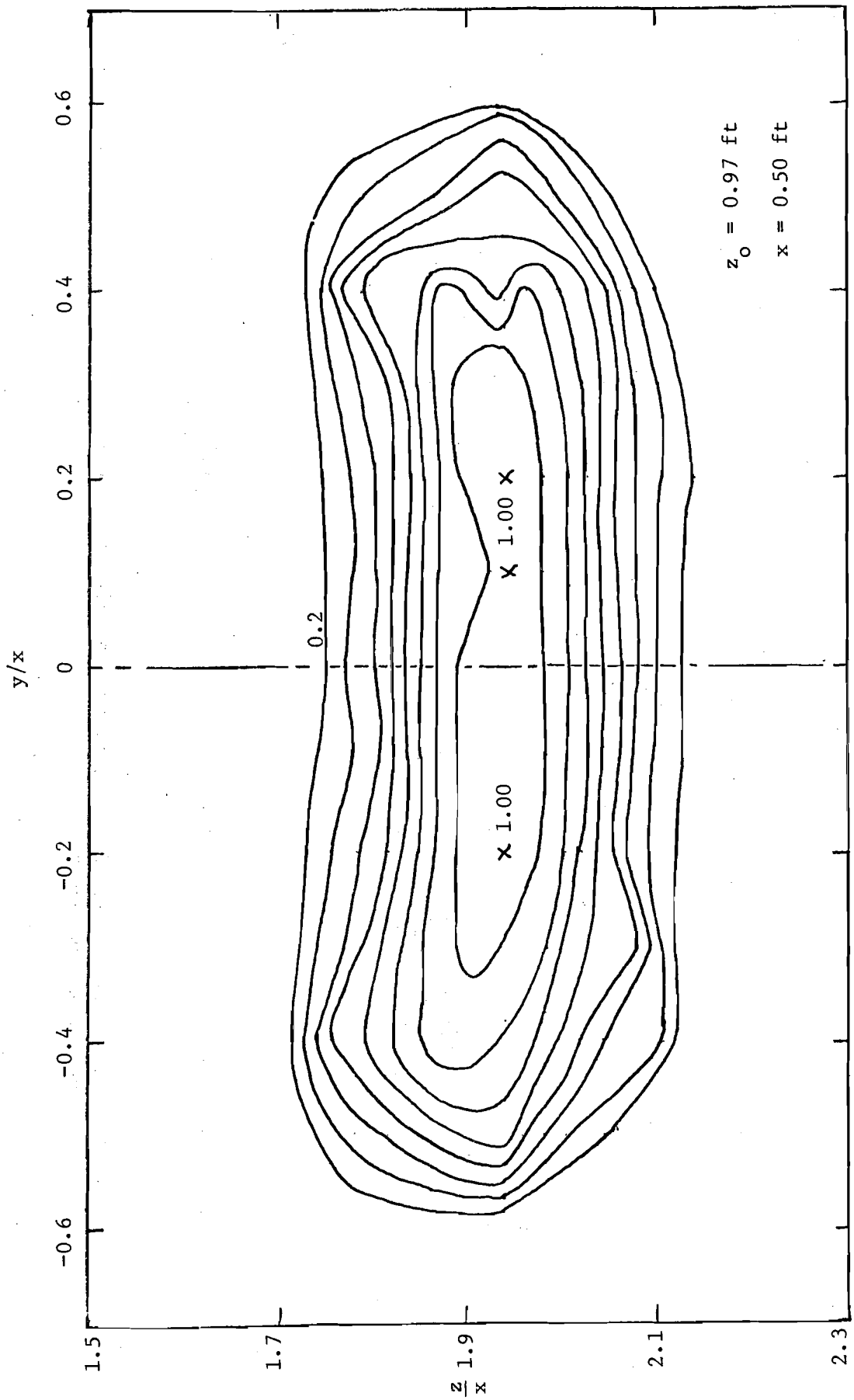

Fig. 8 Isovelocity pattern for unconfined slot discharge submerged 0.97 ft at 0.50 ft downstream from outlet

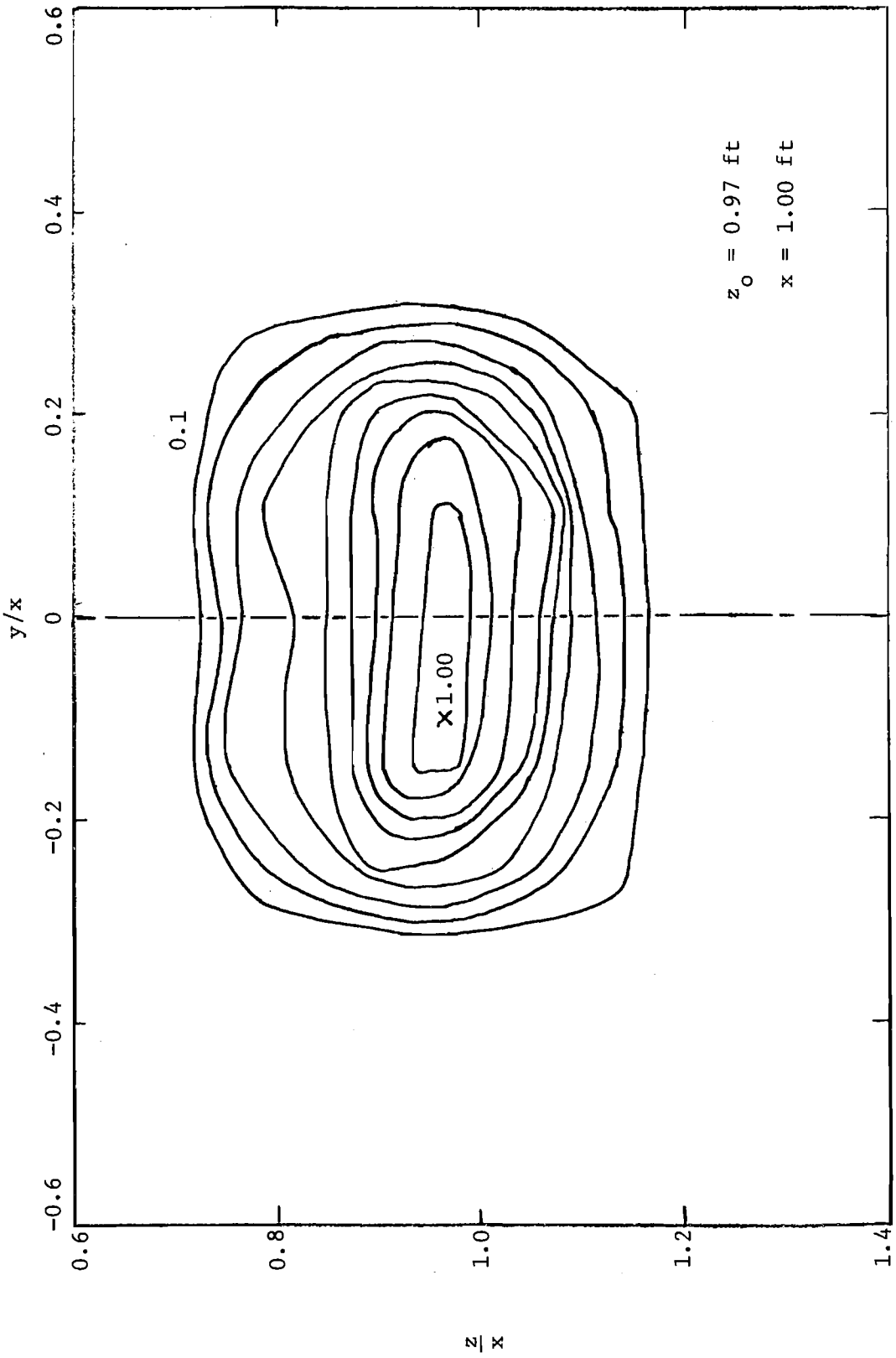

Fig. 9 Isovelocity pattern for unconfined slot discharge submerged 0.97 ft at 1.00 ft downstream from outlet

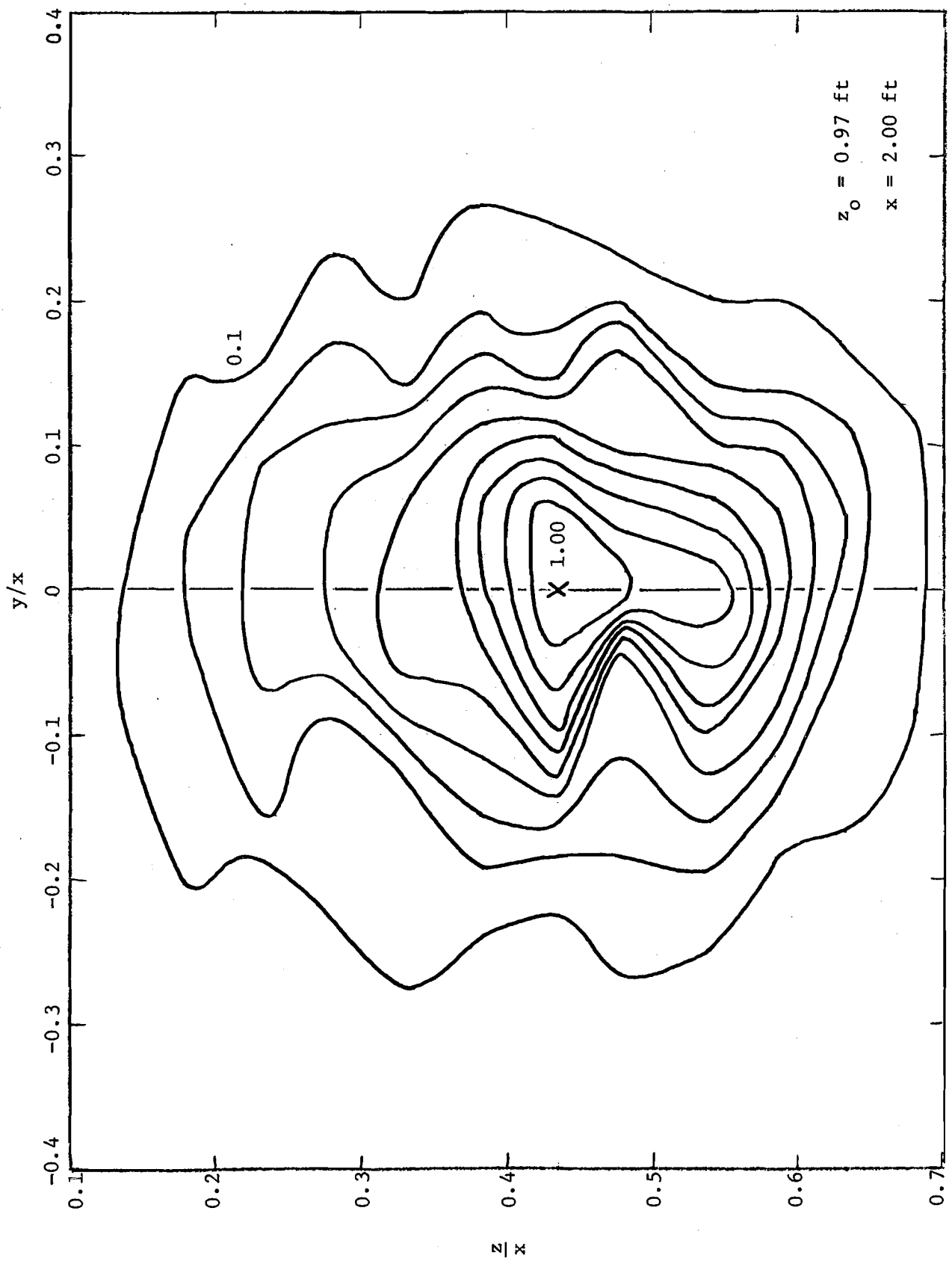

Fig. 10 Isovelocity pattern for unconfined slot discharge submerged 0.97 ft at 2.00 ft downstream from outlet

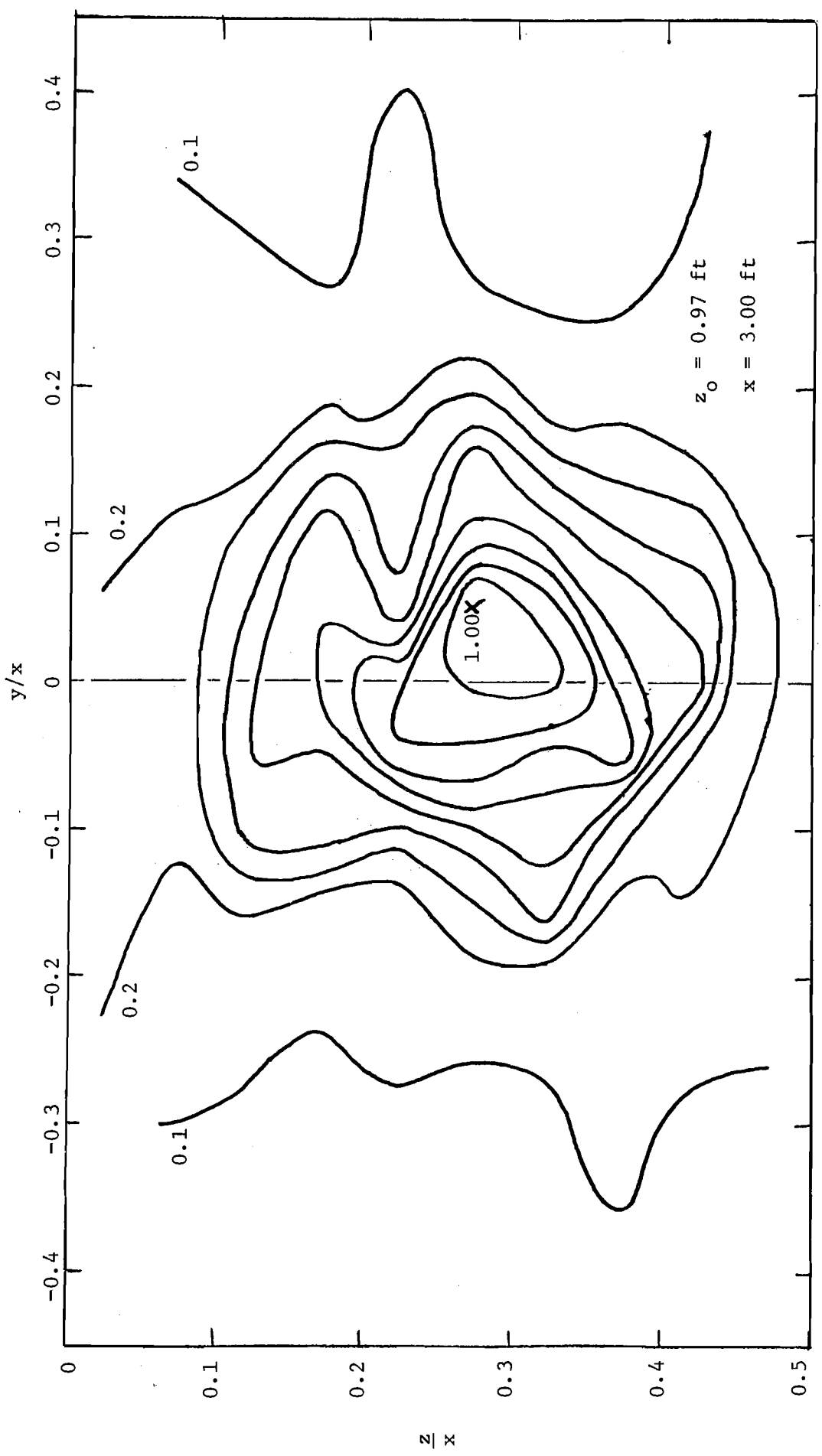

Fig. 11 Isovelocity pattern for unconfined slot discharge submerged 0.97 ft at 3.00 ft downstream from outlet

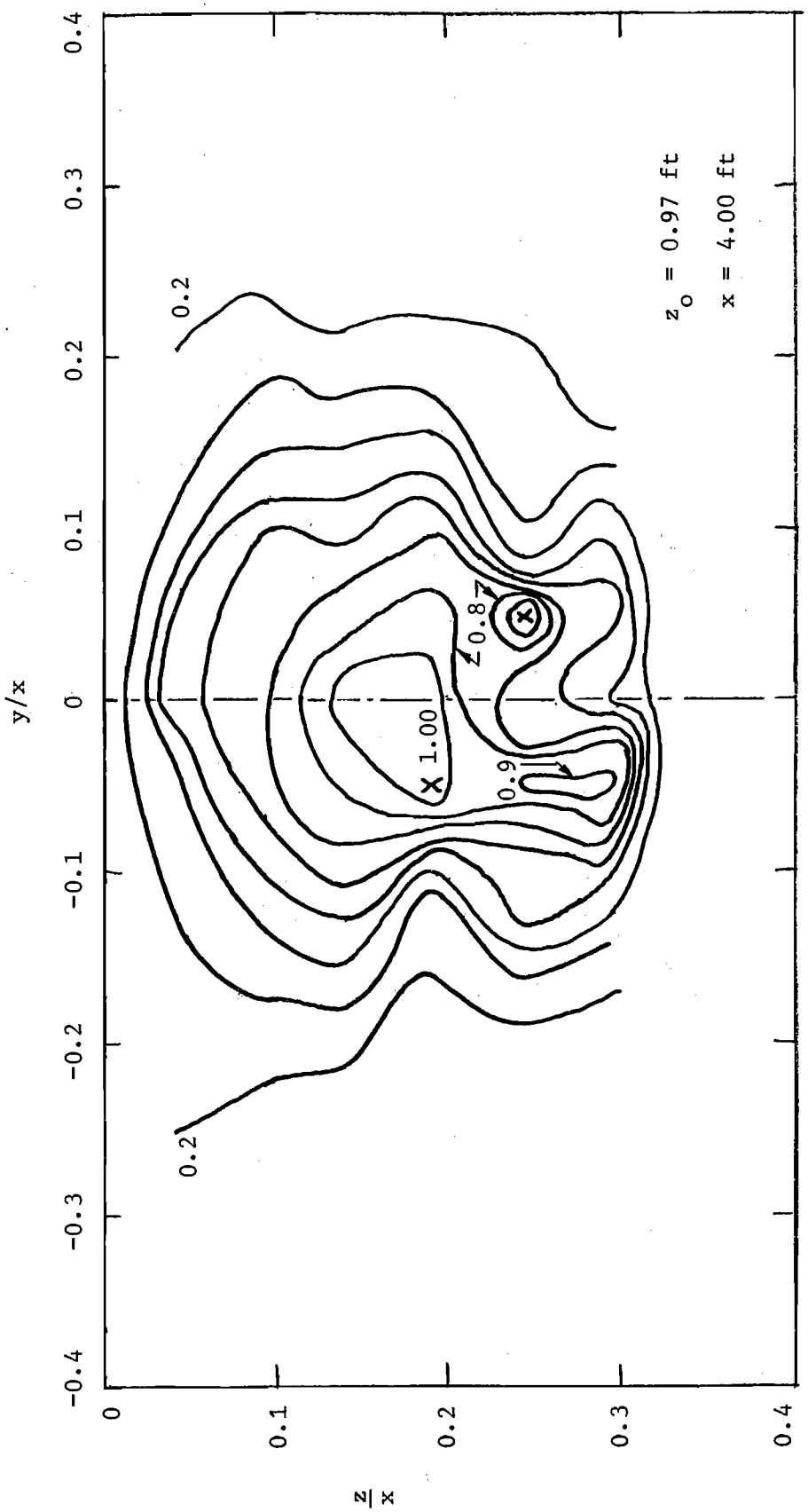

Fig. 12 Isovelocity pattern for unconfined slot discharge submerged 0.97 ft at 4.00 ft downstream from outlet

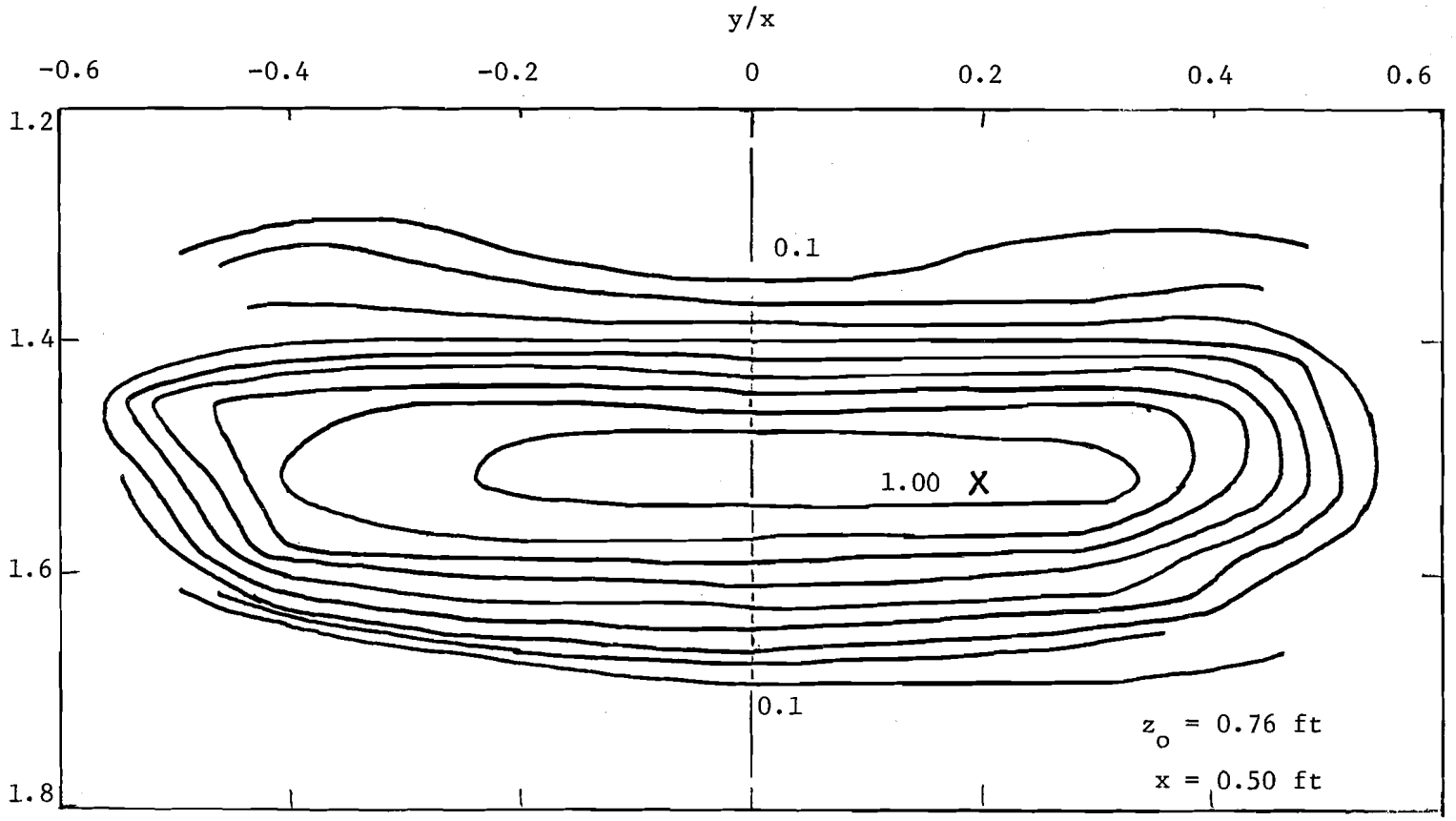

Fig. 13 Isovelocity pattern for unconfined slot discharge submerged 0.76 ft at 0.50 ft downstream from outlet

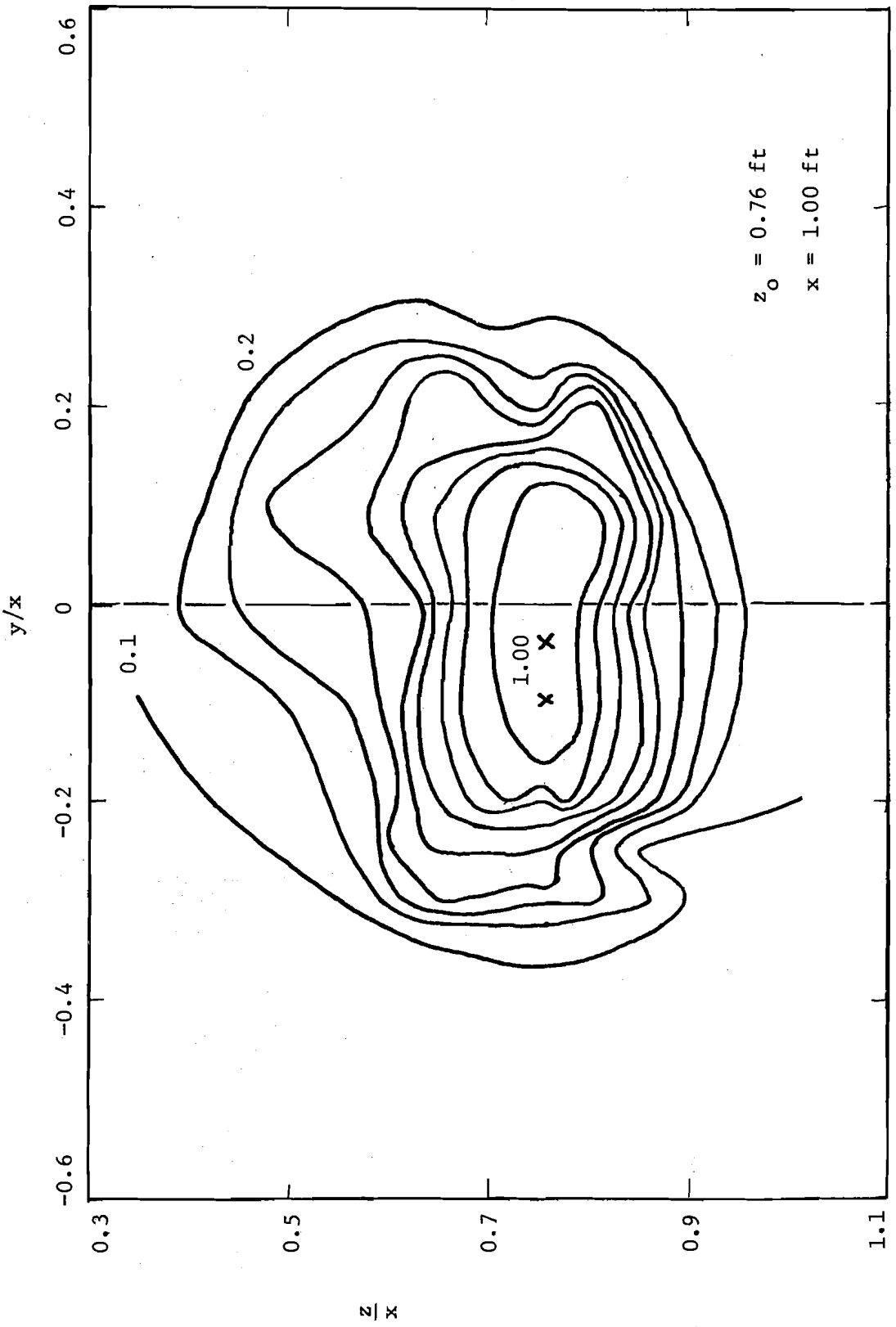

Fig. 14 Isovelocity pattern for unconfined slot discharge submerged 0.76 ft at 1.00 downstream from outlet

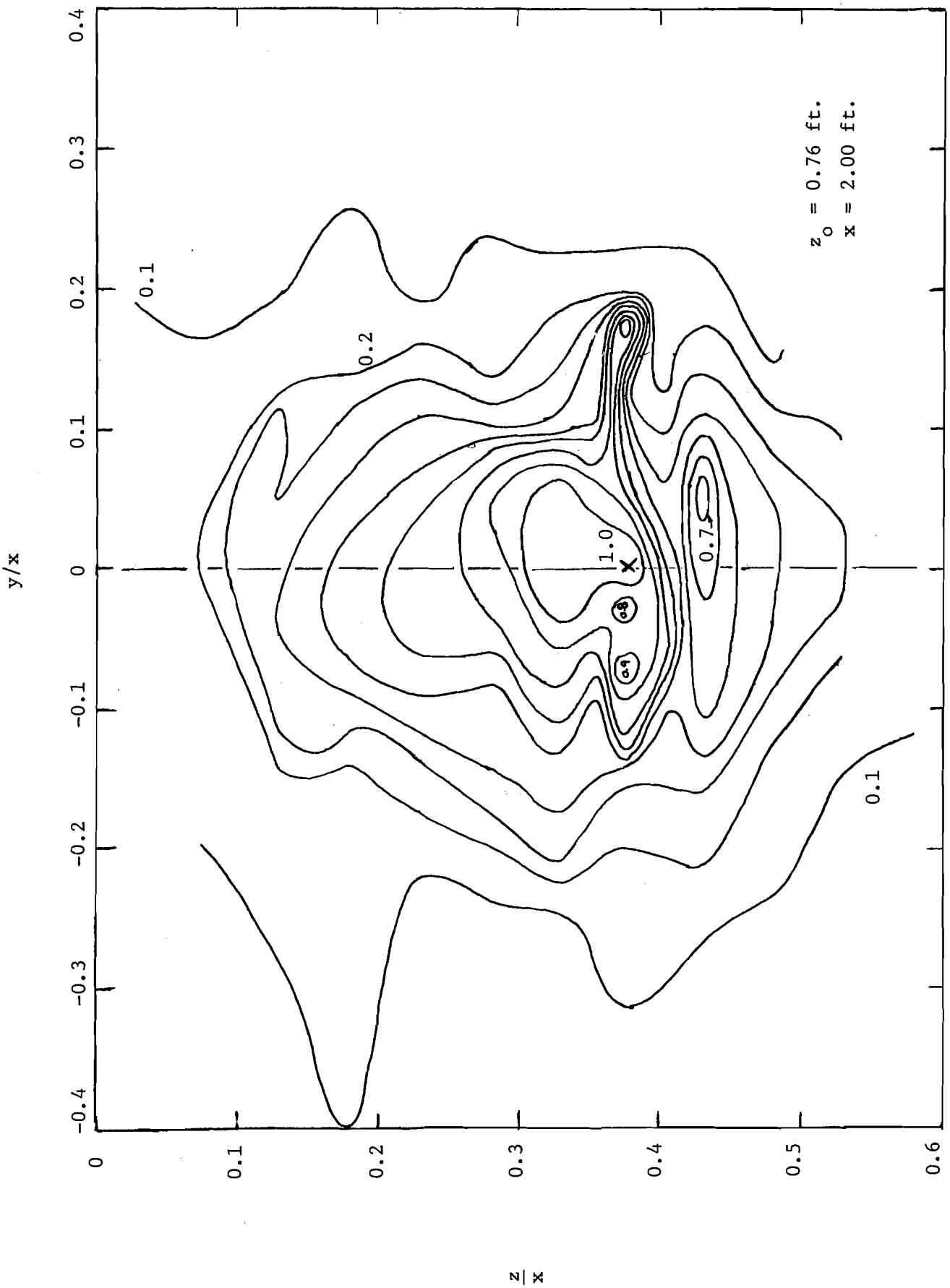

Fig. 15 Isovelocity pattern for unconfined slot discharge submerged 0.76 ft at 2.00 ft downstream from outlet

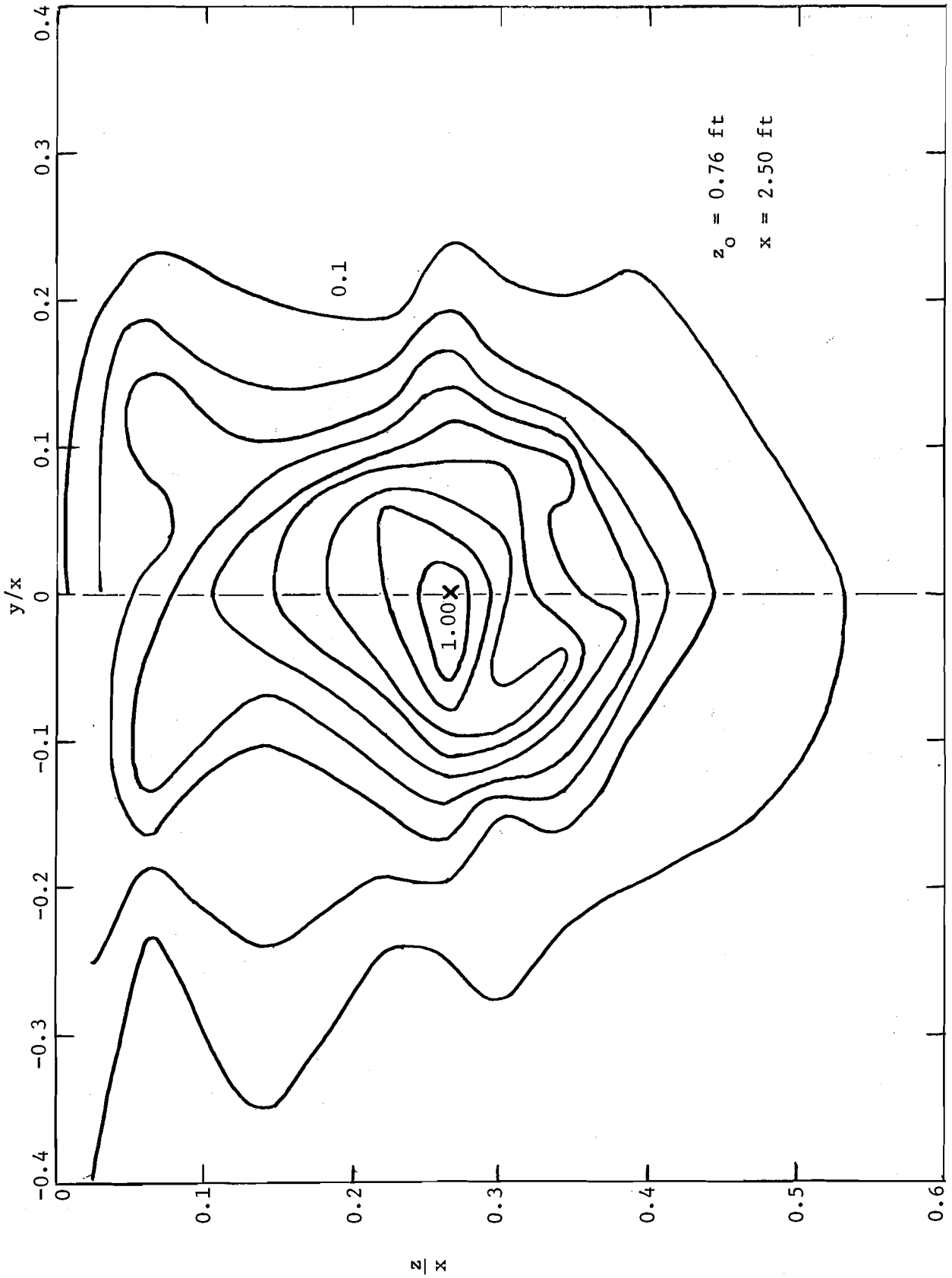

Fig. 16 Isovelocity pattern for unconfined slot discharge submerged 0.76 ft at 2.50 ft downstream from outlet

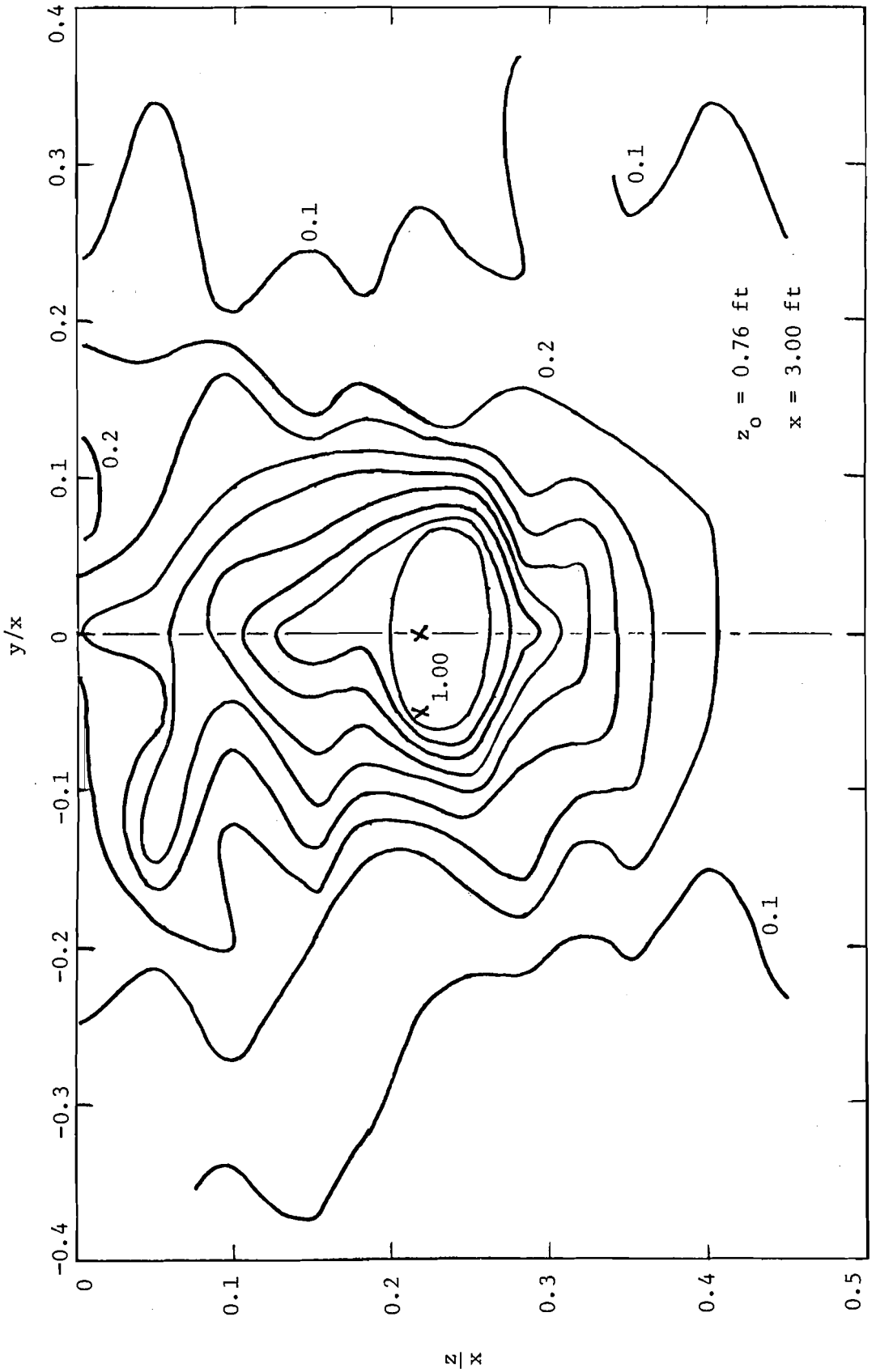

Fig. 17 Isovelocity pattern for unconfined slot discharge submerged 0.76 ft at 3.00 ft downstream from outlet

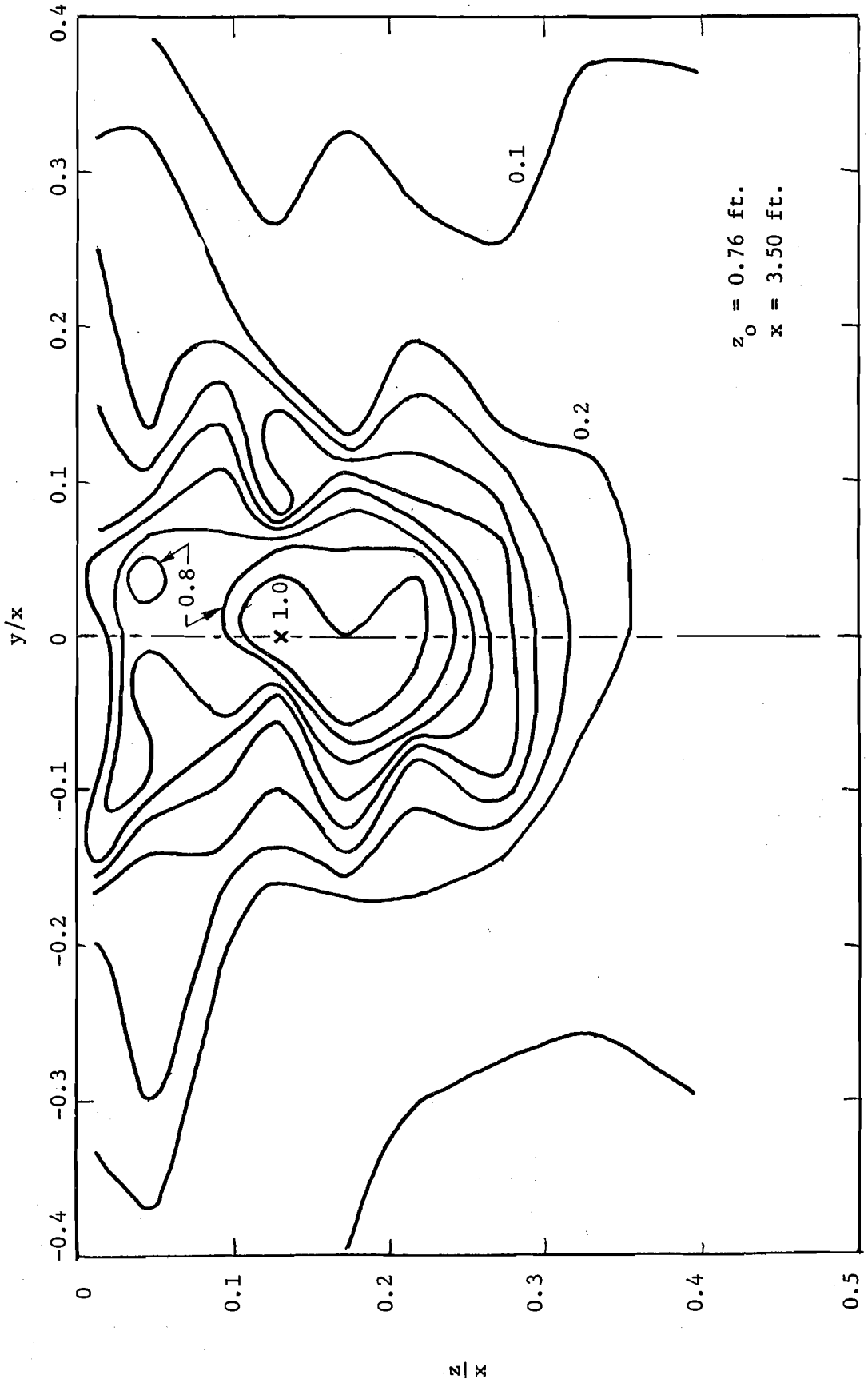

Fig. 18 Isovelocity pattern for unconfined slot discharge submerged 0.76 ft at 3.50 ft downstream from outlet.

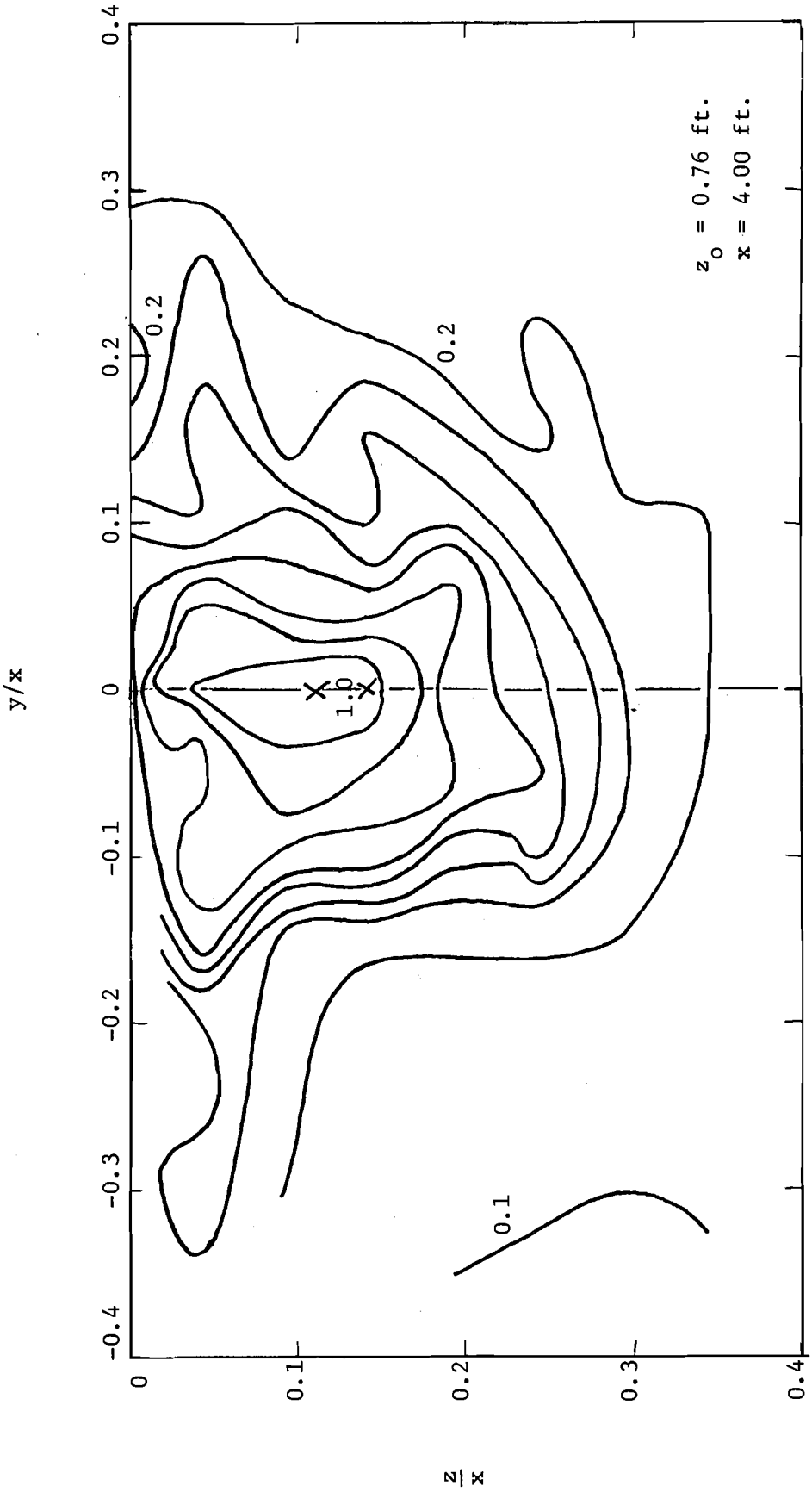

Fig. 19 Isovelocity pattern for unconfined slot discharge submerged 0.76 ft at 4.00 ft downstream from outlet

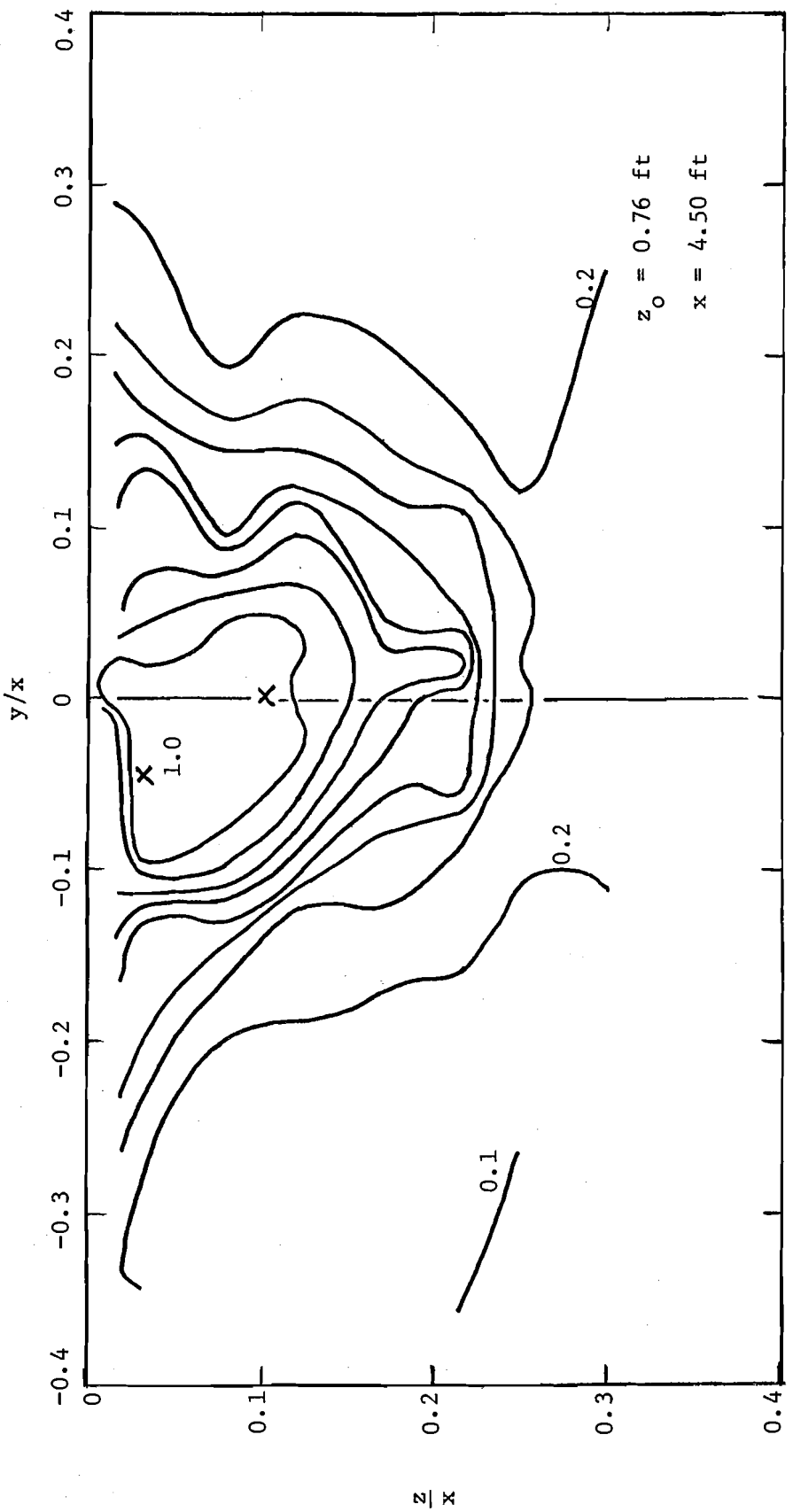

Fig. 20 Isovelocity pattern for unconfined slot discharge submerged 0.76 ft at 4.50 ft downstream from outlet

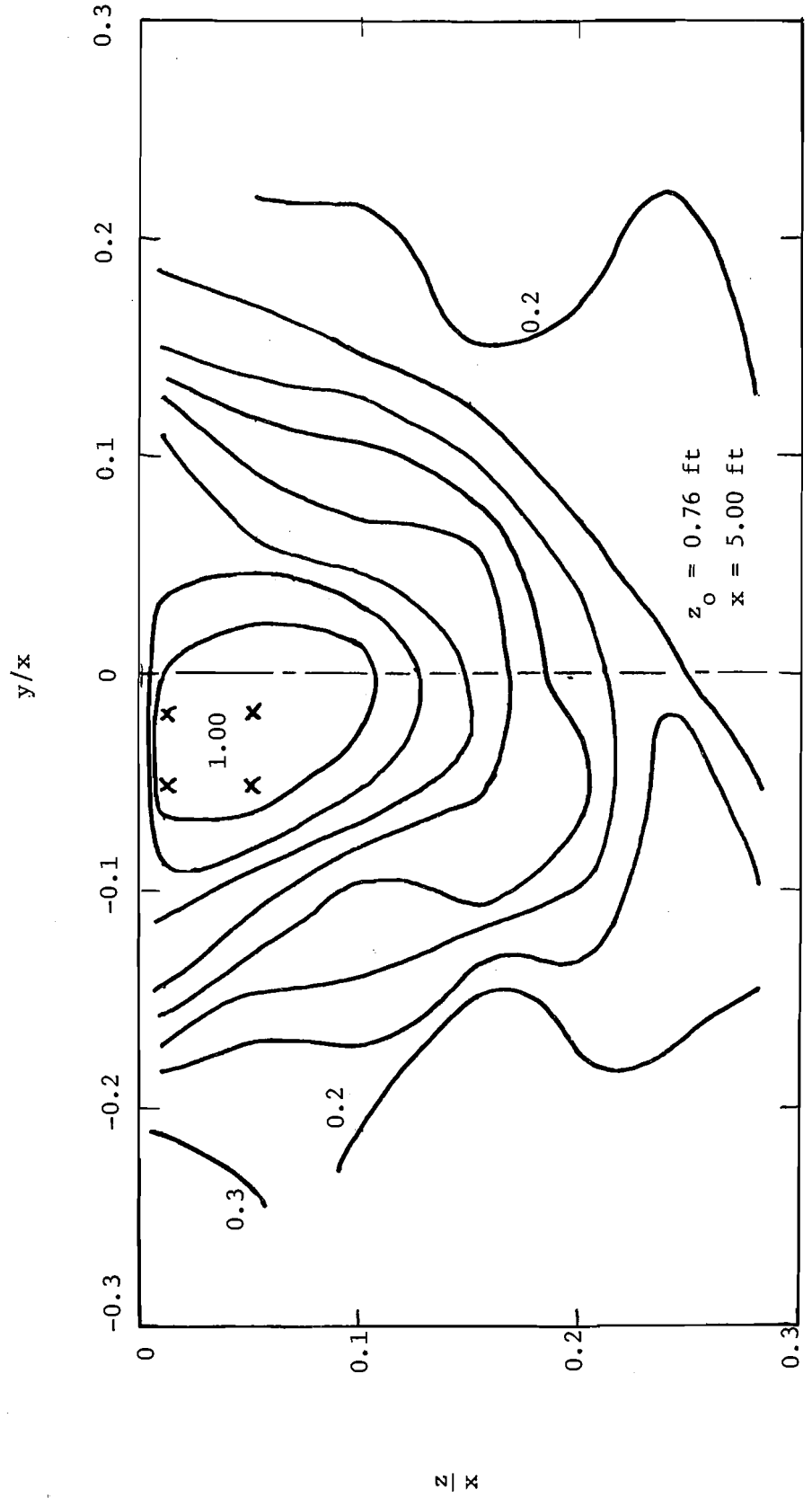

Fig. 21 Isovelocity pattern for unconfined slot discharge submerged 0.76 ft at 5.00 ft downstream from outlet

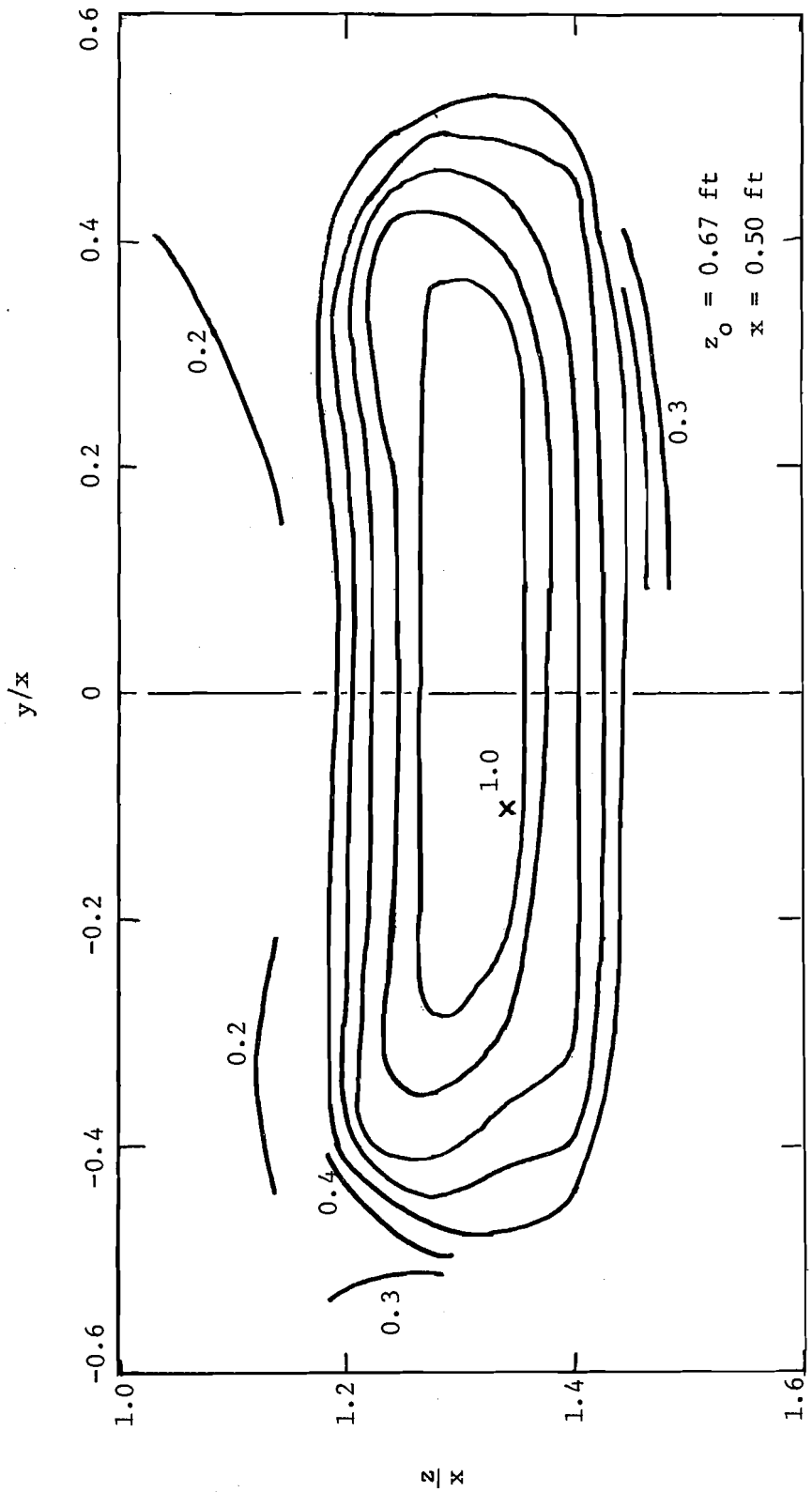

Fig. 22 Isovelocity pattern for unconfined slot discharge submerged 0.67 ft at 0.50 ft downstream from outlet

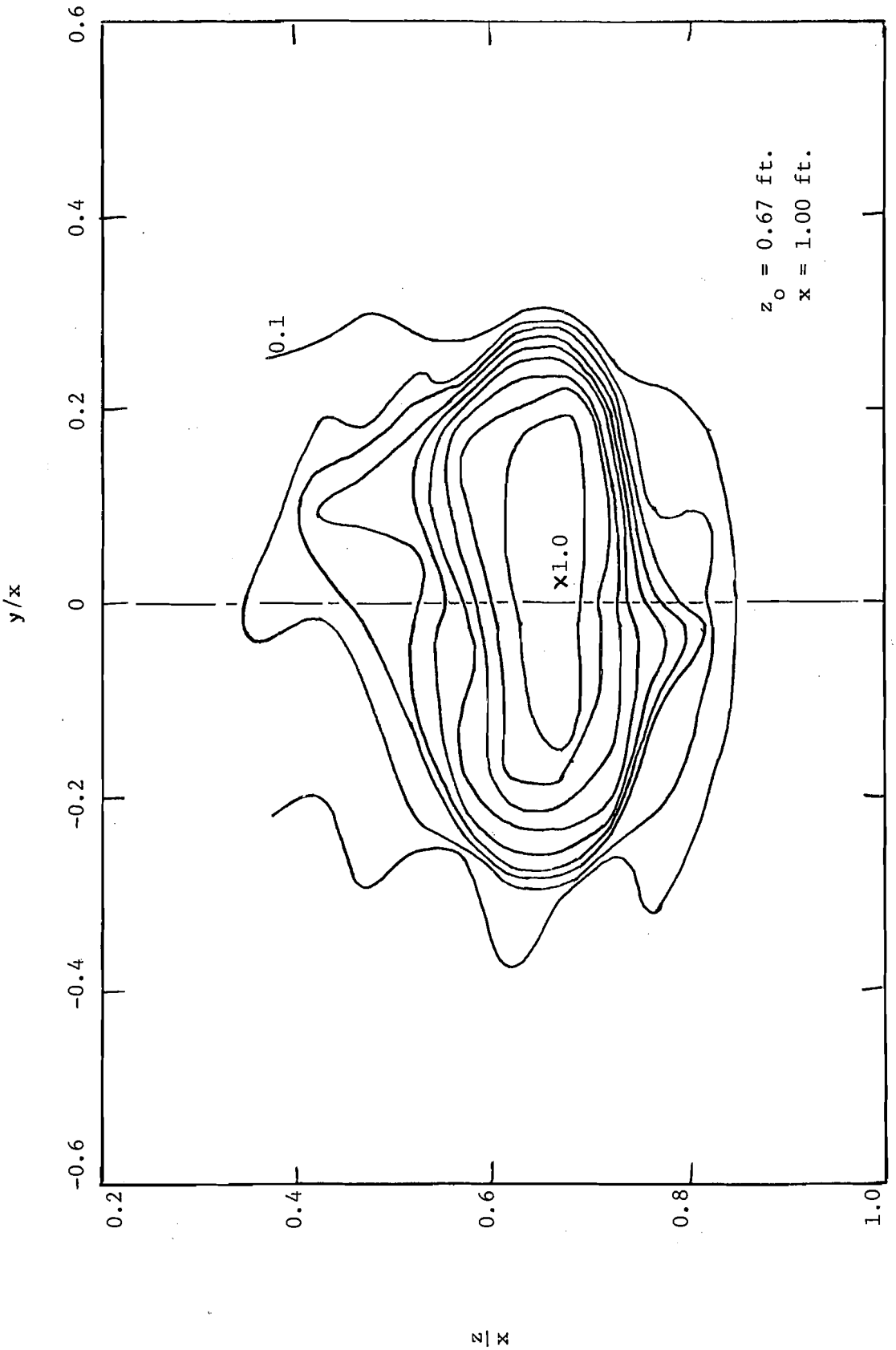

Fig. 23 Isovelocity pattern for unconfined slot discharge submerged 0.67 ft at 1.00 ft downstream from outlet

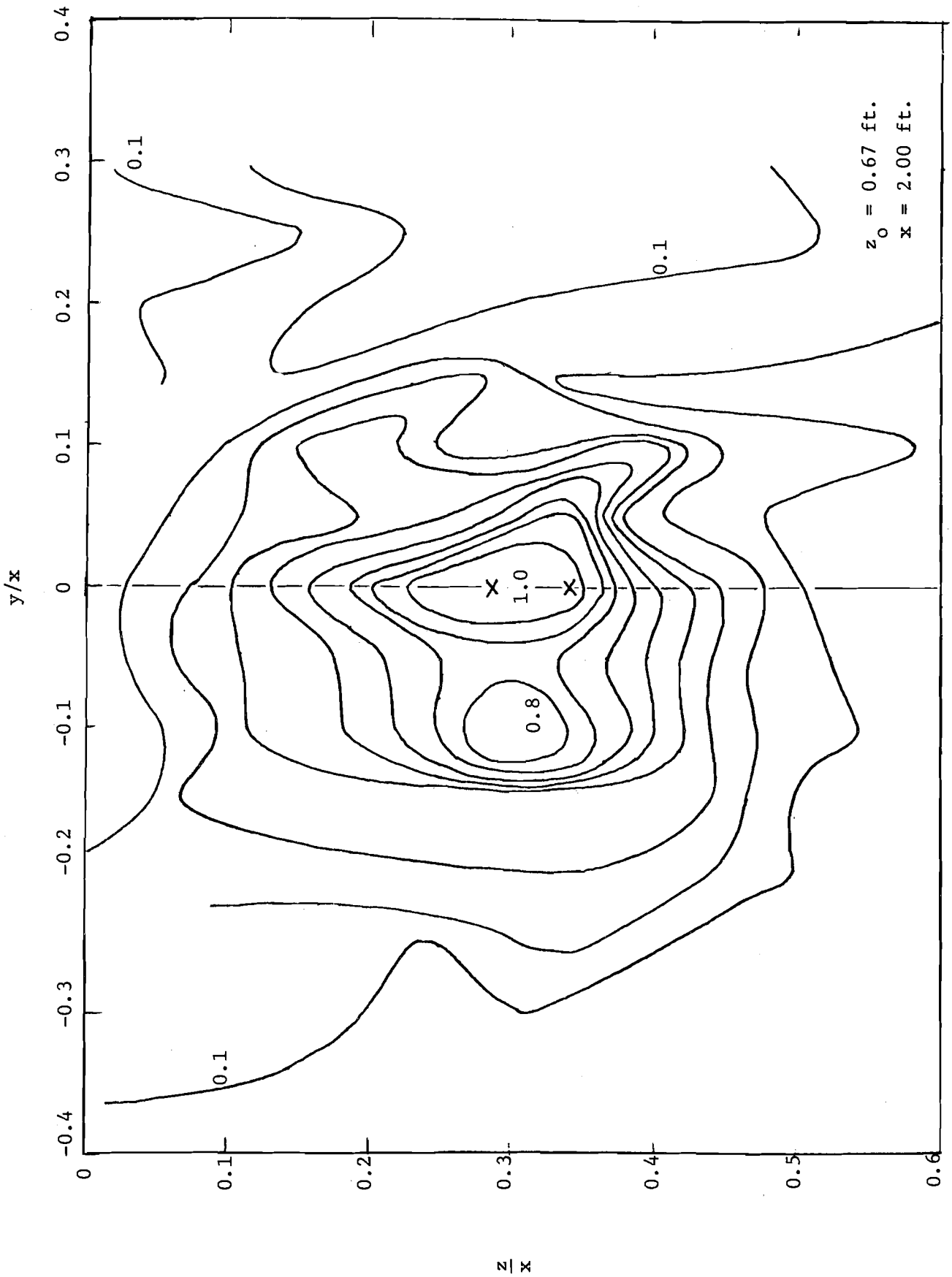

Fig. 24 Isovelocity pattern for unconfined slot discharge submerged 0.67 ft at 2.00 ft downstream from outlet

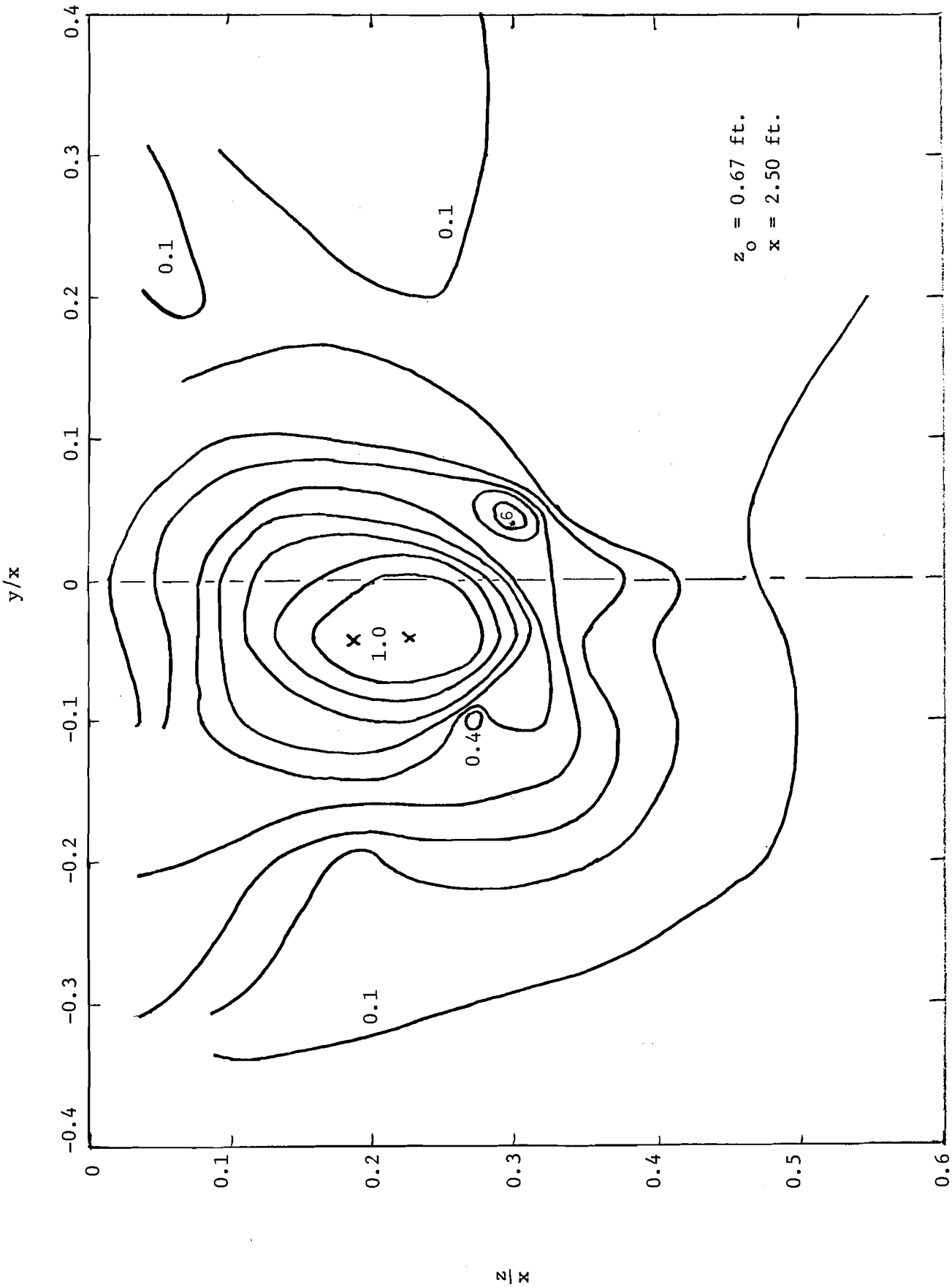

Fig. 25 Isovelocity pattern for unconfined slot discharge submerged 0.67 ft at 2.50 ft downstream from outlet

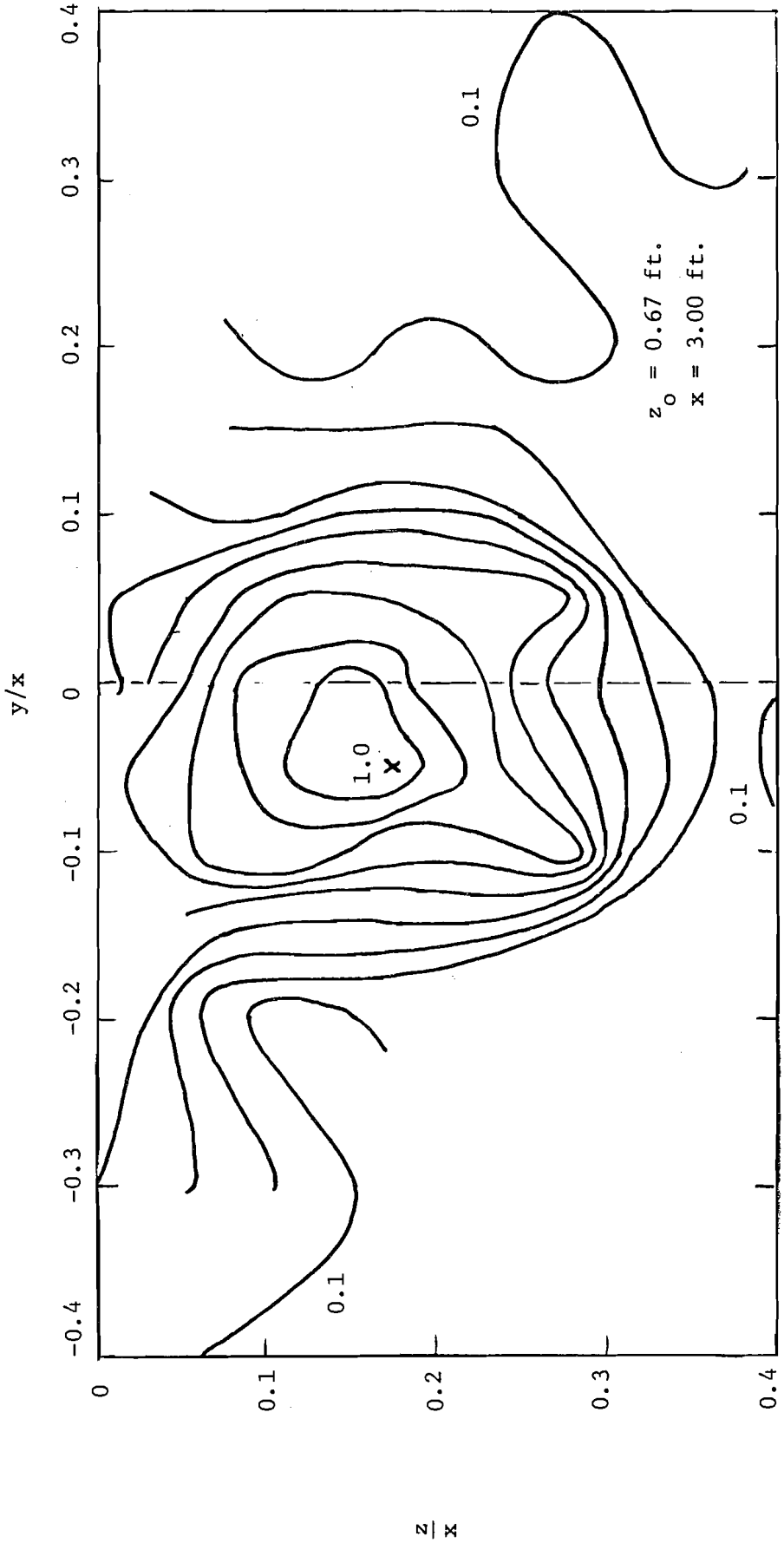

Fig. 26 Isovelocity pattern for unconfined slot discharge submerged 0.67 ft at 3.00 ft downstream from outlet

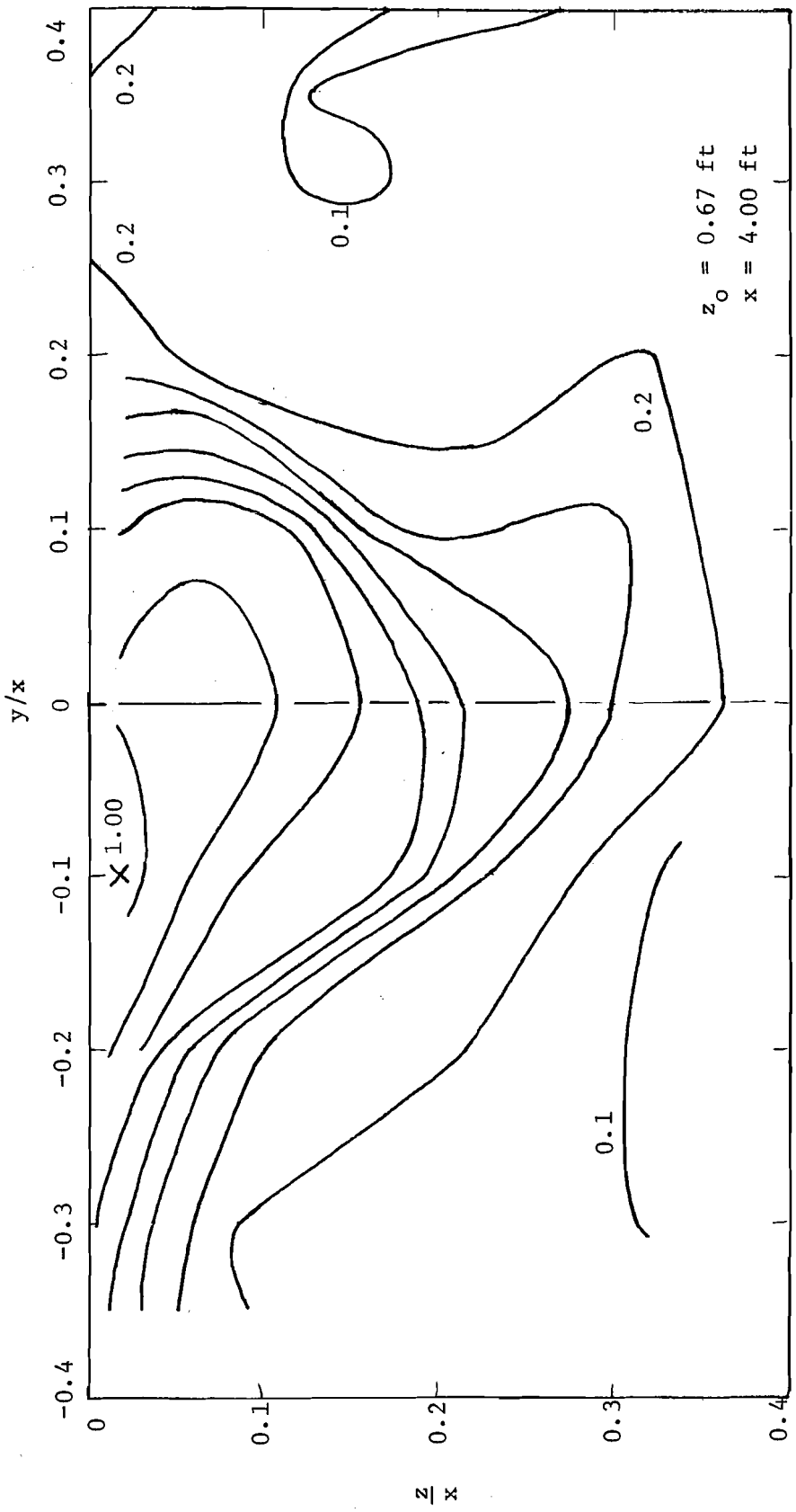

Fig. 27 Isovelocity pattern for unconfined slot discharge submerged 0.67 ft at 4.00 ft downstream from outlet

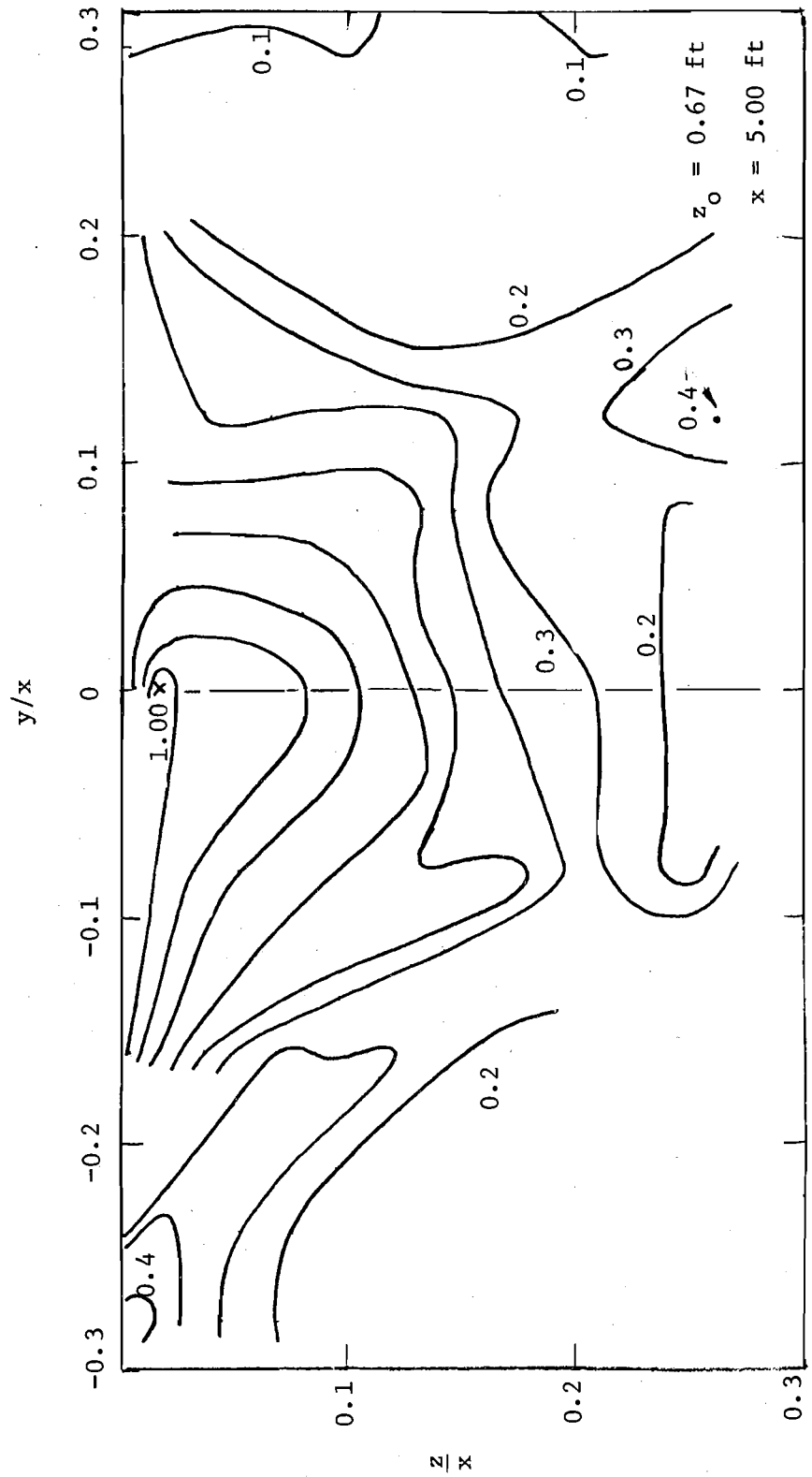

Fig. 28 Isovelocity pattern for unconfined slot discharge submerged 0.67 ft at 5.00 ft downstream from outlet

the behavior of other configurations by tracing the maximum velocity's vertical location using vertical centerline traverses at various longitudinal distances downstream from the outlet. Figure 29 shows a replotting of Fig. 3 including the information on location of maxima contained in Figs. 6 through 28 plus additional information from vertical centerline traverses at other slot submergences. Figure 29 shows that the experimental data for the 1/8-in. by 6-in. slot do not agree with the analysis for the infinitely wide slot, nor does the data collapse to a unique curve for all submergences. Nevertheless, there is substantial influence of the wing-walls on maximum velocity location, although the effect of providing entrainment in the zone above the outlet is somewhat less than that predicted by the plane-symmetric analysis.

Table 1 provides a summary of the tests for which complete isovelocity profiles were obtained. Table 2 summarizes the data for unheated discharges without wing-walls for which the maximum velocity was traced using centerline traverses alone. It should be noted that the values of u_m in Table 2 are the values of the maximum longitudinal velocity for the centerline section, whereas those listed in Table 1 are the maxima for the entire cross section.

III-2. Discharges with Complete Wing-walls

Data collected by John, Mahajan and Kanbour (2) indicated that for a submergence of 1 ft the maximum velocity for the discharge from a 1/8-in. by 6-in. slot set at the head end of a 6-in. channel reached the free surface at a distance of 1.5-ft downstream from the origin. It was therefore decided, in the present investigation, to limit the maximum submergence to 1-ft and to extend the wing-walls in the downstream direction for a distance of 2-ft. With the top of the sidewalls set above the

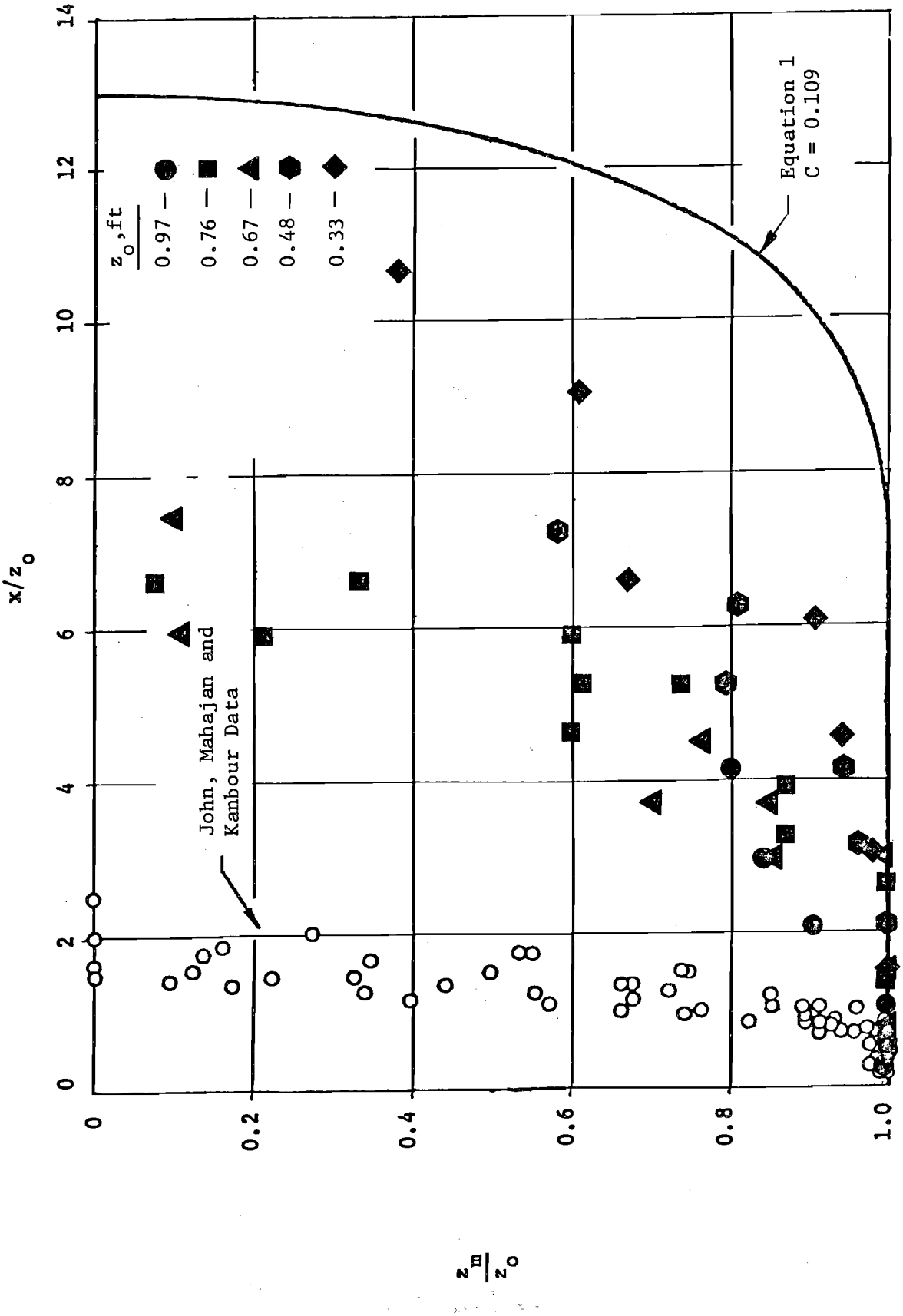

Fig. 29 Location of maximum velocity for unconfined slot discharges compared with Equation 1 and data for confined slot

TABLE 1 - Cold Water Discharges without Wing-walls, Complete Traverses

z_o, ft	x, ft	u_o, ft/sec	u_m, ft/sec	Figure No.	z_m/z_o
0.97	0.20	29.34	19.72	6	0.99
	0.40	32.10	14.05	7	1.00
	0.50	32.10	12.47	8	1.00
	1.00	32.10	9.34	9	1.00
	2.00	31.31	3.93	10	0.90
	3.00	31.31	2.73	11	0.84
	4.00	31.87	1.96	12	0.80
0.76	0.50	31.13	12.74	13	1.00
	1.00	32.10	9.08	14	1.00
	2.00	31.31	4.02	15	1.00
	2.50	31.31	3.59	16	0.87
	3.00	31.31	2.99	17	0.87
	3.50	31.31	2.48	18	0.60
	4.00	31.31	2.13	19	0.61,0.74
	4.50	31.31	2.05	20	0.21,0.60
	5.00	31.31	1.96	21	0.08,0.34
0.67	0.50	31.44	12.20	22	1.00
	1.00	31.31	7.63	23	1.00
	2.00	30.35	3.93	24	0.85,1.00
	2.50	30.52	3.24	25	0.70,0.85
	3.00	30.69	2.82	26	0.77
	4.00	30.52	1.96	27	0.11
	5.00	30.69	2.22	28	0.10

TABLE 2 - Cold Water Discharges Without Wing-walls, Vertical Centerline Traverses

z_o, ft	x, ft	u_o ft/sec	u_m ft/sec	z_m/z_o
0.48	0.5	30.78	12.28	1.00
	1.0		8.61	1.00
	1.5		7.12	0.96
	2.0		5.81	0.94
	2.5		4.87	0.79
	3.0		4.21	0.81
	3.5		3.75	0.58
0.33	0.5	30.78	12.31	1.00
	1.0		9.01	0.97
	1.5		6.98	0.94
	2.0		5.98	0.91
	2.5		4.83	0.67
	3.0		4.11	0.61
	3.5		3.81	0.38

free surface this was expected to cut off entrainment on the upper side of the nozzle and effectively reproduce the results obtained by John et al. For cold water discharges an initial attempt was made to conduct the investigation with outlet velocities having the same order of magnitude as when the wing-walls were absent (approximately 30 ft/sec.). However, with the wing-walls in place this resulted in unstable pulsating behavior with submergence of the outflow only occurring on an intermittent basis. In order to avoid this phenomenon the outlet velocity was reduced to about 8 ft/sec, the value used by John et al. The problem of stability of the flow pattern is dealt with in more detail in a later section. As a consequence of the reduction in velocity it was necessary to use the Kent Type 265 current meter system exclusively for the measurements. In order to check that the behavior was the same as that obtained by John et al. the maximum velocity was traced for the conditions summarized in Table 3 by taking vertical centerline velocity traverses. The maxima locations obtained from these traverses are plotted in Figure 30, with b = slot height (1/8-in.) The data show good agreement with that of John et al. and again there is no significant difference between the heated and unheated discharge behavior.

TABLE 3 - Tests with Complete Wing-walls, Vertical Center-line Velocity Traverses

z_o, ft.	U_o, ft/sec.	ΔT, F°	T_H, °F
0.97	8.31	0	-
0.97	8.40	22	99
0.76	8.31	0	-
0.48	8.31	0	-
0.33	8.31	0	-
0.33	8.56	28	98

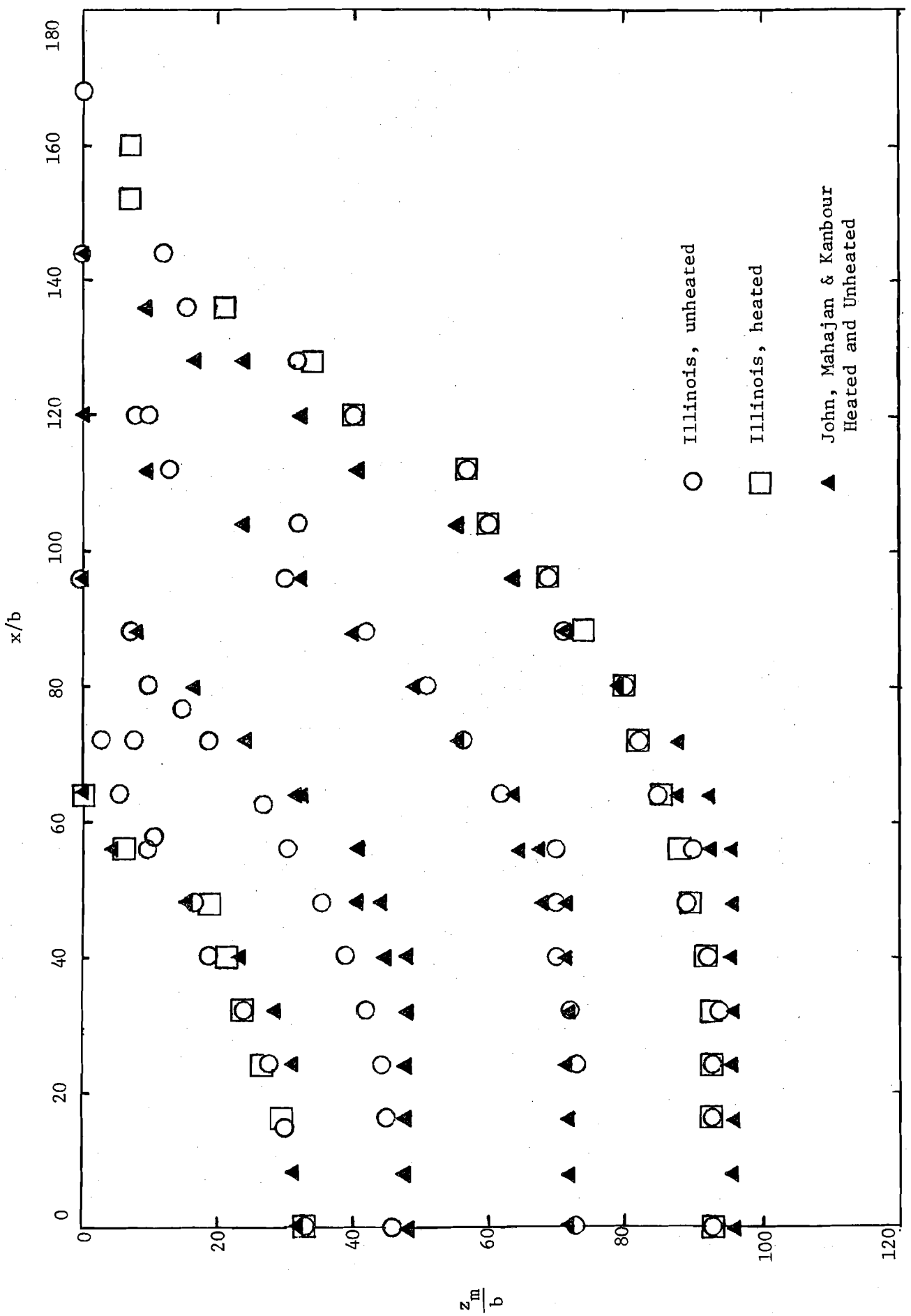

Fig. 30 Maximum velocity location for heated and unheated discharges between complete wing-walls for several submergences

III-3. Cold Water Additions to Trapped Vortex Zone

Since it was anticipated that it would be difficult, if not impossible in the time available, to measure the entrainment due to openings in the wing-walls or due to flow over the top of the wing-walls an initial attempt was made to measure the behavior when cold water was added independently to the trapped vortex zone above the slot outlet. The method of addition is illustrated schematically in Figure 31. Cold make-up water was introduced through a 2-in. pipe submerged just below the undisturbed free surface and ending about 1 in. in front of the wall. The maximum discharge necessary was estimated by using the entrainment calculated for a 6-in. width of a wide two-dimensional unconfined jet outlet. The make-up water discharge was measured using an orifice meter in the 2-in. line. This was calibrated in situ using the 10° V-notch weir used to measure slot discharges. It was found that before sufficient make-up water could be added to satisfy the entrainment estimated for an infinitely submerged slot that the flow pattern was dominated by the make-up water discharge since this was generally larger than the slot discharge. As the make-up water discharge approached 0.16 cfs the slot discharge deflected sharply upwards, apparently attracted by the larger discharge introduced on top. Figure 32 shows the results for lesser make-up water discharges for a submergence of the slot equal to 0.97 ft. The slot discharge, Q_o, for all of these tests was 0.0427 cfs. Q_a = the added discharge. The open symbols represent the locations of the maximum for unheated slot discharges whereas the darkened symbols show locations for heated discharges as indicated on the figure. For comparison the results of the previous tests both with and without complete wing-walls are included. The measurements show that for added discharges up to about twice the

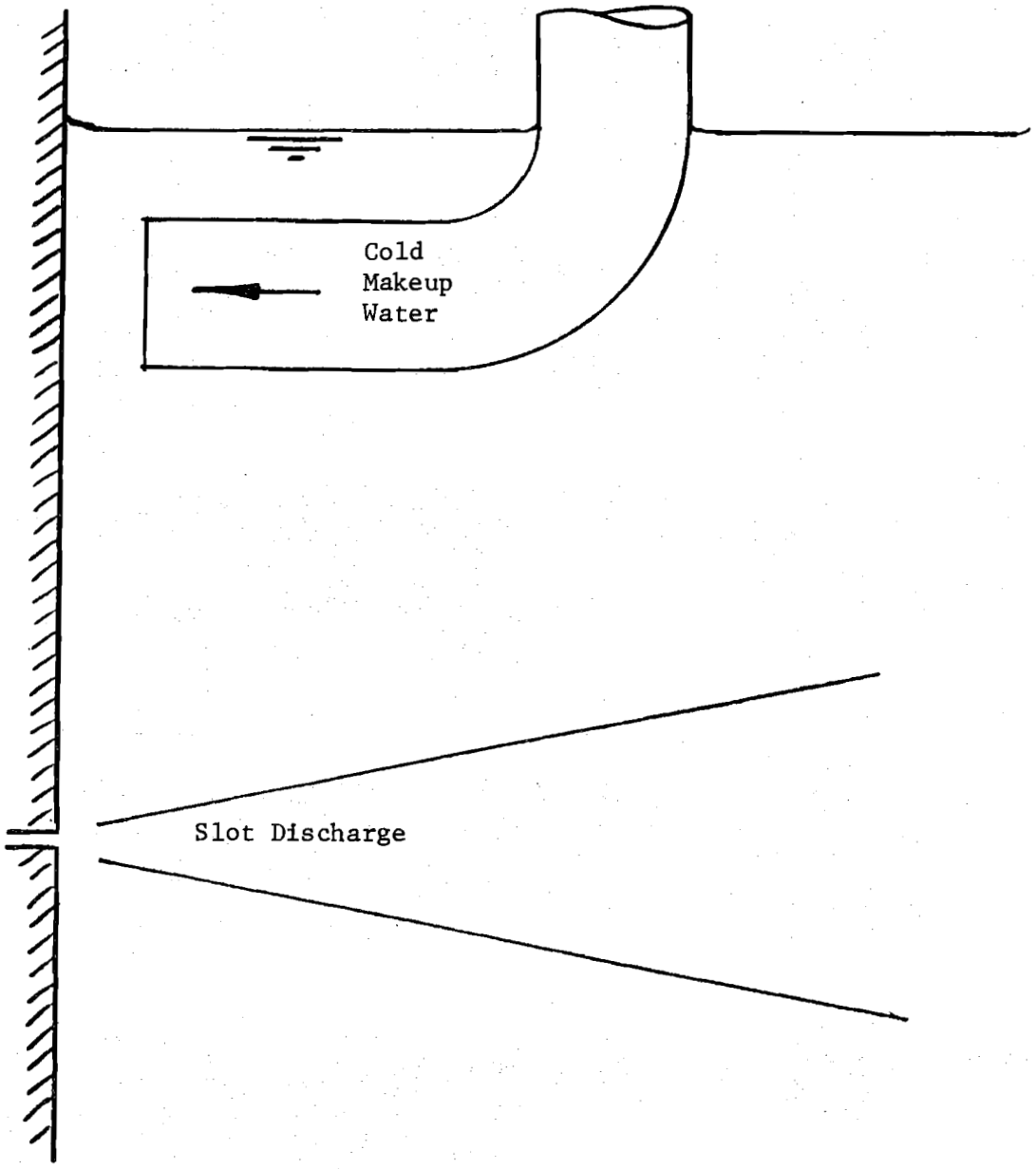

Fig. 31 Schematic representation of method used to add cold water to trapped vortex zone

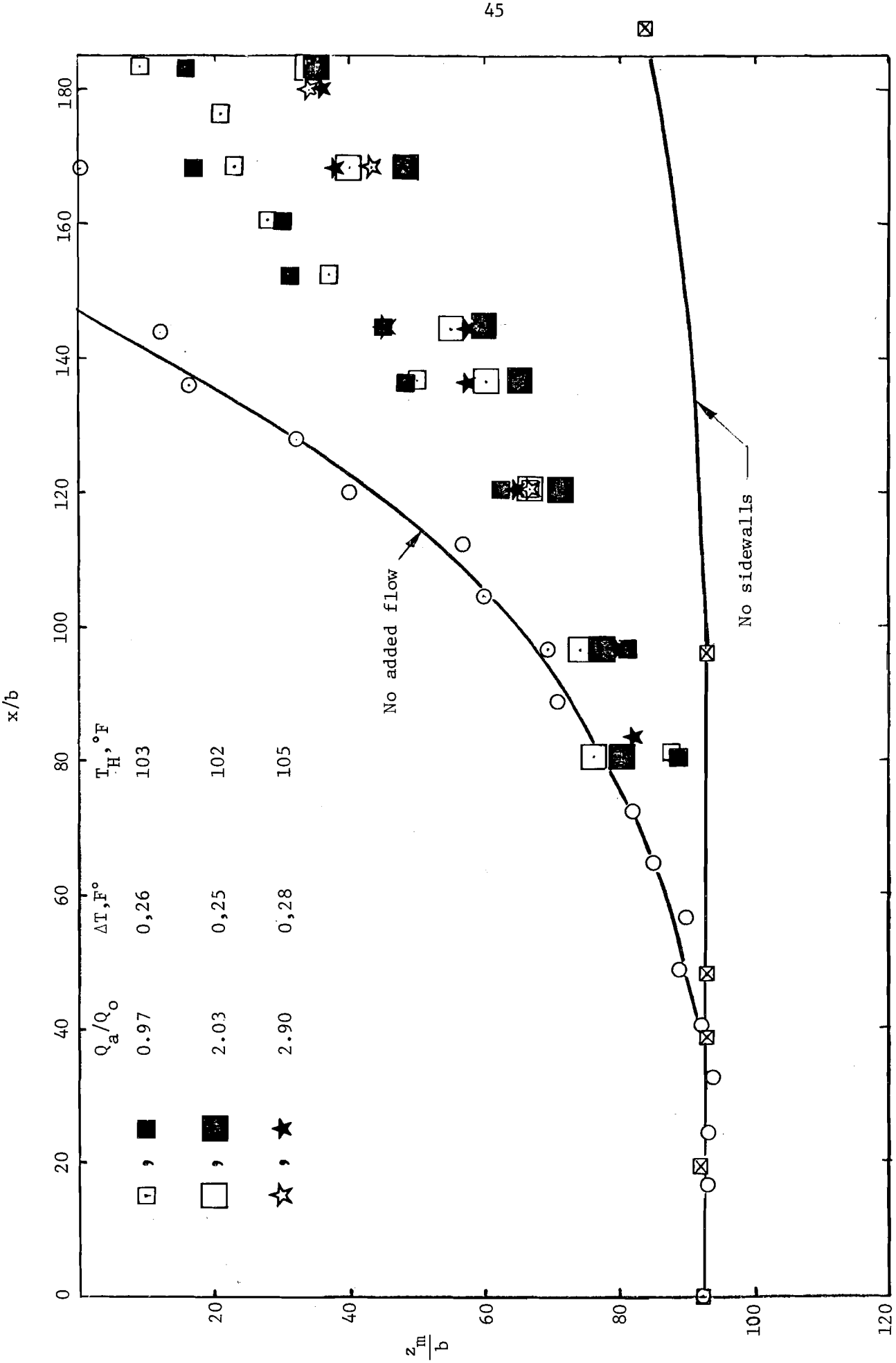

Fig. 32 Location of maximum velocity for various additions of cold water to trapped vortex zone for submergence of 0.97 ft

slot discharge there is a trend from the behavior with no added flow toward that when sidewalls are absent. It is thought that the failure to move further toward the no-sidewall behavior with the use of further addition of flow is caused by the tendency of the added flow to assume the character of a surface jet which utilizes the slot discharge as entrainment rather than vice versa. It was concluded, therefore, that this aspect of the investigation should not be pursued further. The data does, however, provide at least qualitative evidence that the flow pattern may be controlled by satisfying the entrainment requirements on the upper side of the slot discharge.

III-4. Variation of Wing-wall Top Elevation

It was decided that a reasonable field configuration for control of inflow to the vortex zone above the slot outlet would involve the use of variable gates set on top of the wing-walls or the use of stop-logs set along the top of the wing-walls. In order to simulate the effect of such means of control in the laboratory without modelling details of the configuration tests were conducted with the top of the wing-walls set at various elevations below the free surface. In all cases tested the crest elevation of both wing-walls was identical. All of the tests described in this section were conducted for a slot submergence of 0.97 ft. For each configuration the location of the maximum velocity was traced using both heated and unheated slot discharges. For heated discharges the location of the maximum temperature was also traced. Cold make-up water was introduced in the reservoir to avoid heat build-up as described in an earlier section. The variation in the location of the maximum for the three different cases is illustrated in Figure 33. The location of the top of the wing-walls is given by z_t which is the vertical distance to the

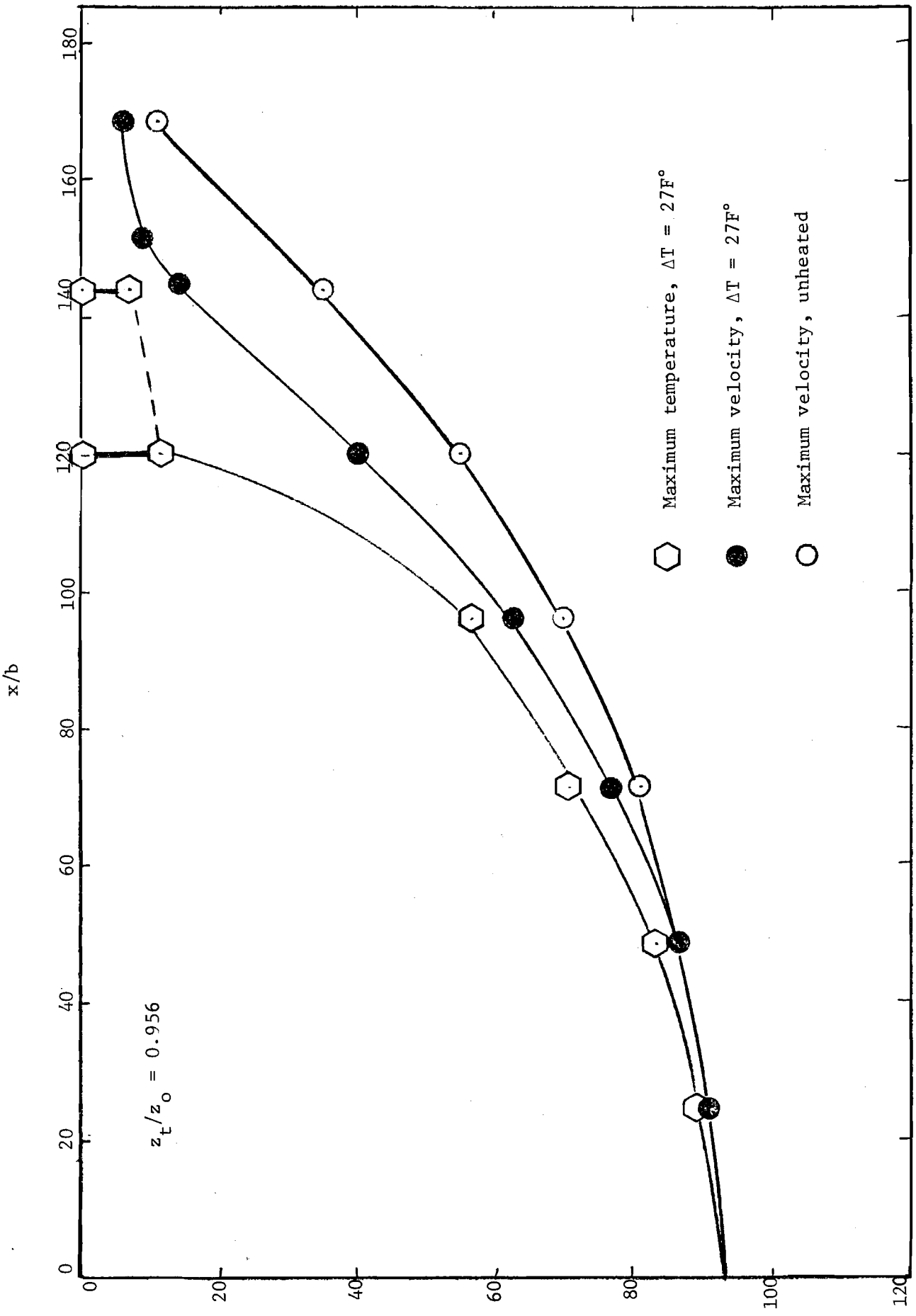

Fig. 33 Variation between locations of various maxima for submerged wing-wall crest and slot submergence of 0.97 ft with L/b = 192

top of the wall from the center line of the slot or, if the wall projects through the free surface, z_t = submergence of the slot. Thus z_t/z_o has a maximum value of 1.000. Figures 34, 35 and 36 show the locations of the maxima for the three different measurements for various locations of the wall top. These figures illustrate that when z_t/z_o is reduced to 0.870 the entrainment requirements of the slot discharge are essentially satisfied and the trace of the maximum is essentially the same as when the wing walls are absent. It is also evident from the figures that the behavior of the flow pattern can be regulated between the limits of complete cut-off and essentially zero cut-off of entrainment by varying the wall (or gate) crest over a fraction of the slot submergence. Since the selection of the wall length in the downstream direction may be somewhat conservative it remains to determine the extent to which the wing-walls may be shortened without losing the capacity to control the flow pattern. Table 4 summarizes the test conditions plotted in Figures 33, 34, 35 and 36.

III.5 Effect of Reducing Wall Length

All of the tests described in this section were again conducted for a slot submergence of 0.97 ft. Two different conditions for z_t/z_o were tested, namely 0.934 and 1.000. The wall length in the downstream x-direction, L, was shortened in increments of 1 1/2 in. and vertical center-line traverses made to locate the point of maximum velocity or maximum temperature for both heated and unheated discharges as summarized in Table 5. There was insufficient time available to test other values of z_t/z_o.

Figures 37, 38 and 39 reproduce the data for unheated and heated velocity and temperature maximum traces for several wall lengths with $z_t/z_o = 0.934$. All three indicate a sudden loss of control of the flow

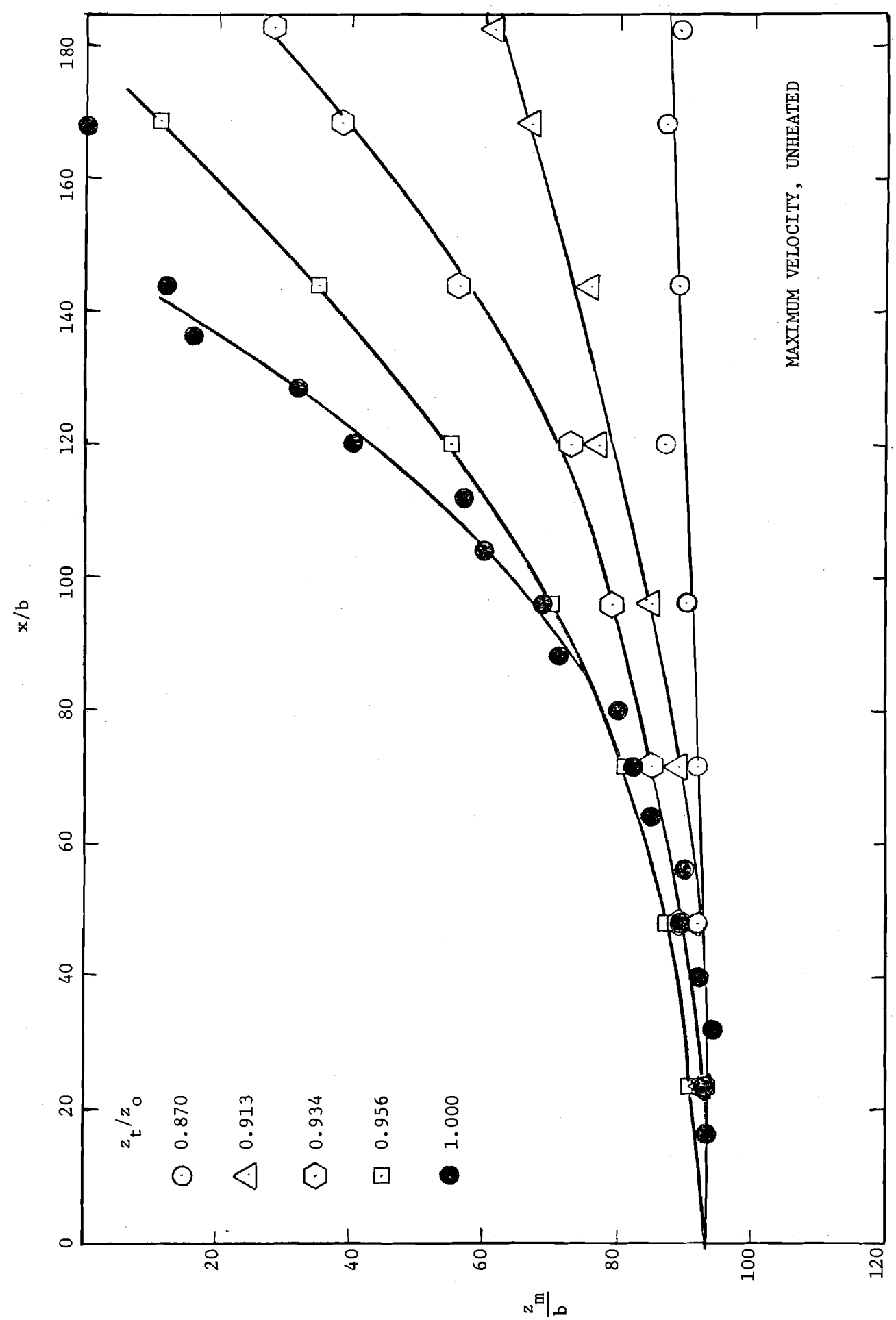

Fig. 34 Location of maximum velocity for unheated discharges between wing-walls with crests at several elevations and slot submergence of 0.97 ft with L/b = 192

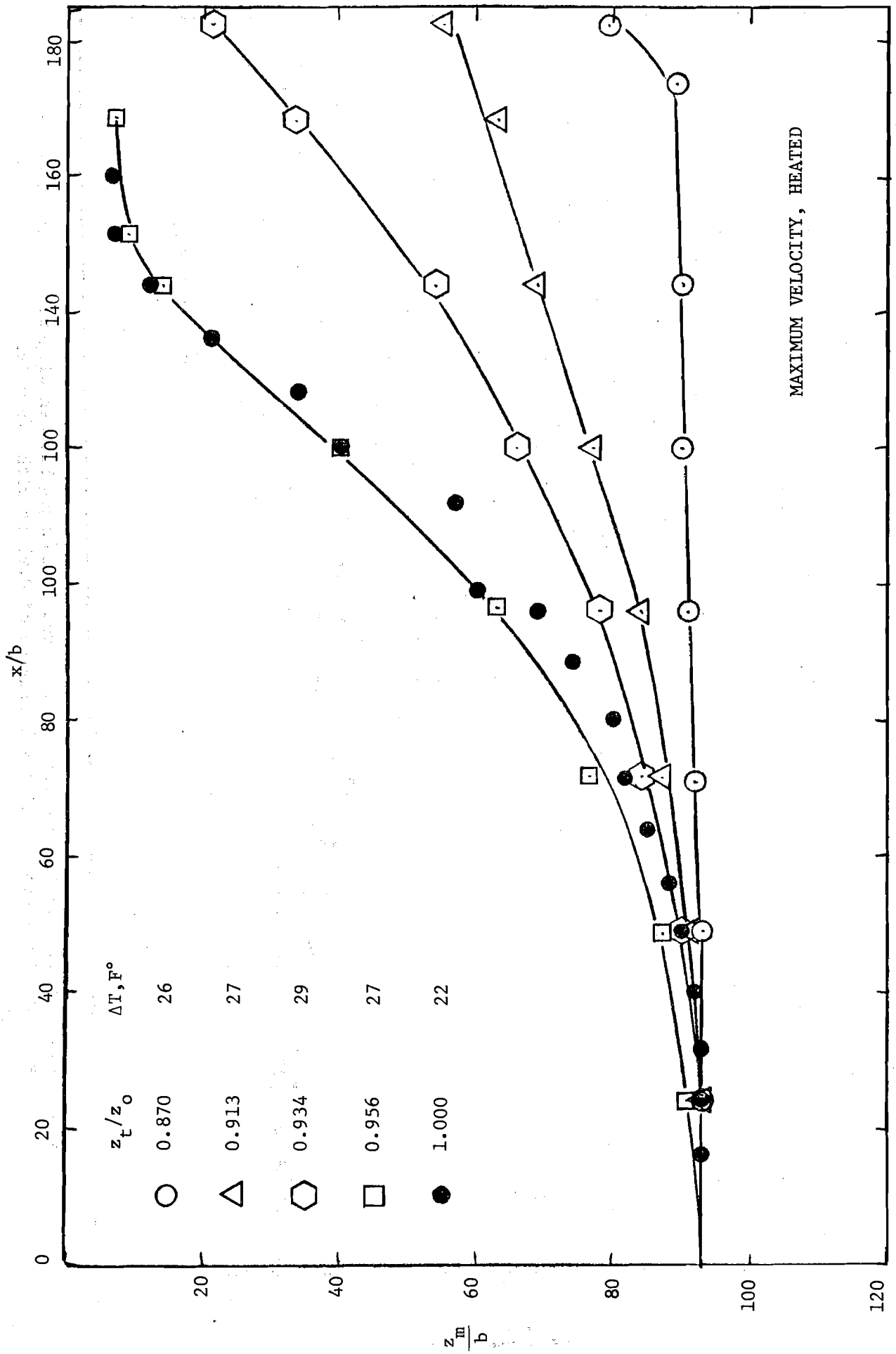

Fig. 35 Location of maximum velocity for heated discharges between wing-walls with crests at several elevations and slot submergence of 0.97 ft with L/b = 192

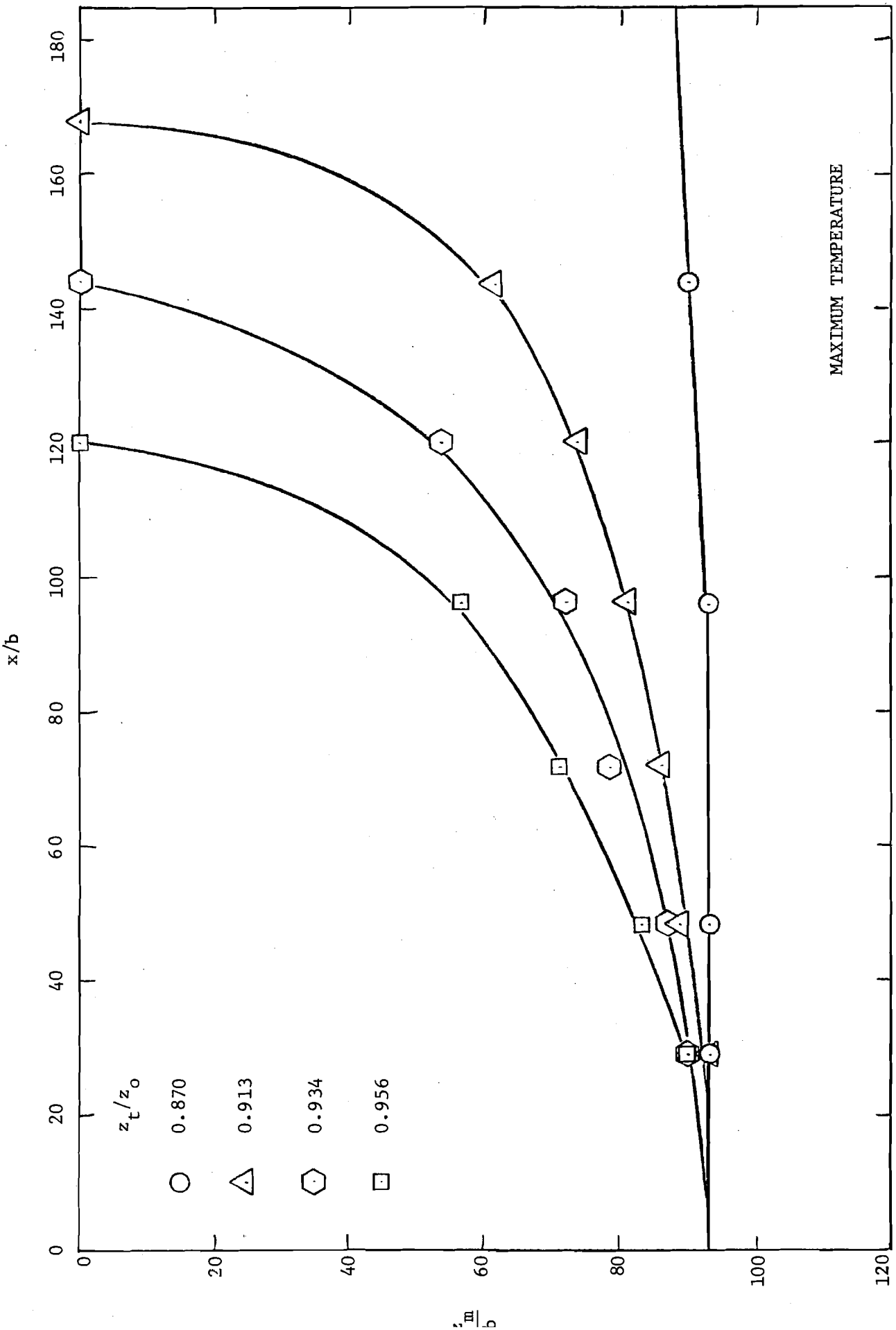

Fig. 36 Location of maximum temperature for heated discharges between wing-walls with crests at several elevations and slot submergence of 0.97 ft with L/b = 192

TABLE 4 - Summary of Tests with Submerged Wing-wall Crest

z_t/z_o	u_o ft/sec	Diffuser Discharge, cfs	ΔT, F°	T_H, °F	Profile Type
0.870	8.24	0.100	27	105	Temperature
	8.39	0.099	0	-	Velocity
	8.39	0.099	26	105	Velocity
0.913	8.28	0.099	28	104	Temperature
	8.20	0.099	0	-	Velocity
	8.24	0.099	27	103	Velocity
0.934	8.16	0.099	28	102	Temperature
	8.24	0.099	0	-	Velocity
	8.24	0.099	29	102	Velocity
0.956	8.28	0.099	28	105	Temperature
	8.35	0.100	0	-	Velocity
	8.35	0.100	27	106	Velocity
1.000	8.31	0	0	-	Velocity
	8.40	0	22	99	Velocity

TABLE 5 - Summary of Tests with Shortened Wing-walls

z_t/z_o	$\frac{L}{b}$	u_o, ft/sec.	Diffuser Discharge, cfs	ΔT, F°	T_H °F	Profile Type
0.934	180	8.63	0.100	0	--	Velocity
	180	8.63	0.100	26	98	Velocity
	180	8.35	0.099	24	95	Temperature
	168	8.20	0.100	0	--	Velocity
	168	8.20	0.100	24	95	Velocity
	168	8.44	0.100	24	95	Temperature
	156	8.23	0.101	0	--	Velocity
	156	6.87	0.101	20	88	Velocity
	156	7.88	0.101	29	96	Temperature
	144	8.35	0.100	0	--	Velocity
	144	7.65	0.099	30	99	Velocity
	144	8.19	0.099	26	96	Temperature
	132	8.31	0.100	0	--	Velocity
	132	8.08	0.101	28	91	Velocity
	132	8.15	0.101	25	92	Temperature
1.000	180	8.52	0.100	0	--	Velocity
	180	8.60	0.095	24	94	Temperature
	156	8.40	0.100	0	--	Velocity
	156	8.08	0.100	28	96	Velocity
	156	8.08	0.101	27	96	Temperature
	144	8.27	0.100	0	--	Velocity
	144	8.27	0.100	28	90	Velocity
	132	8.31	0.100	0	--	Velocity
	132	8.31	0.099	29	93	Velocity

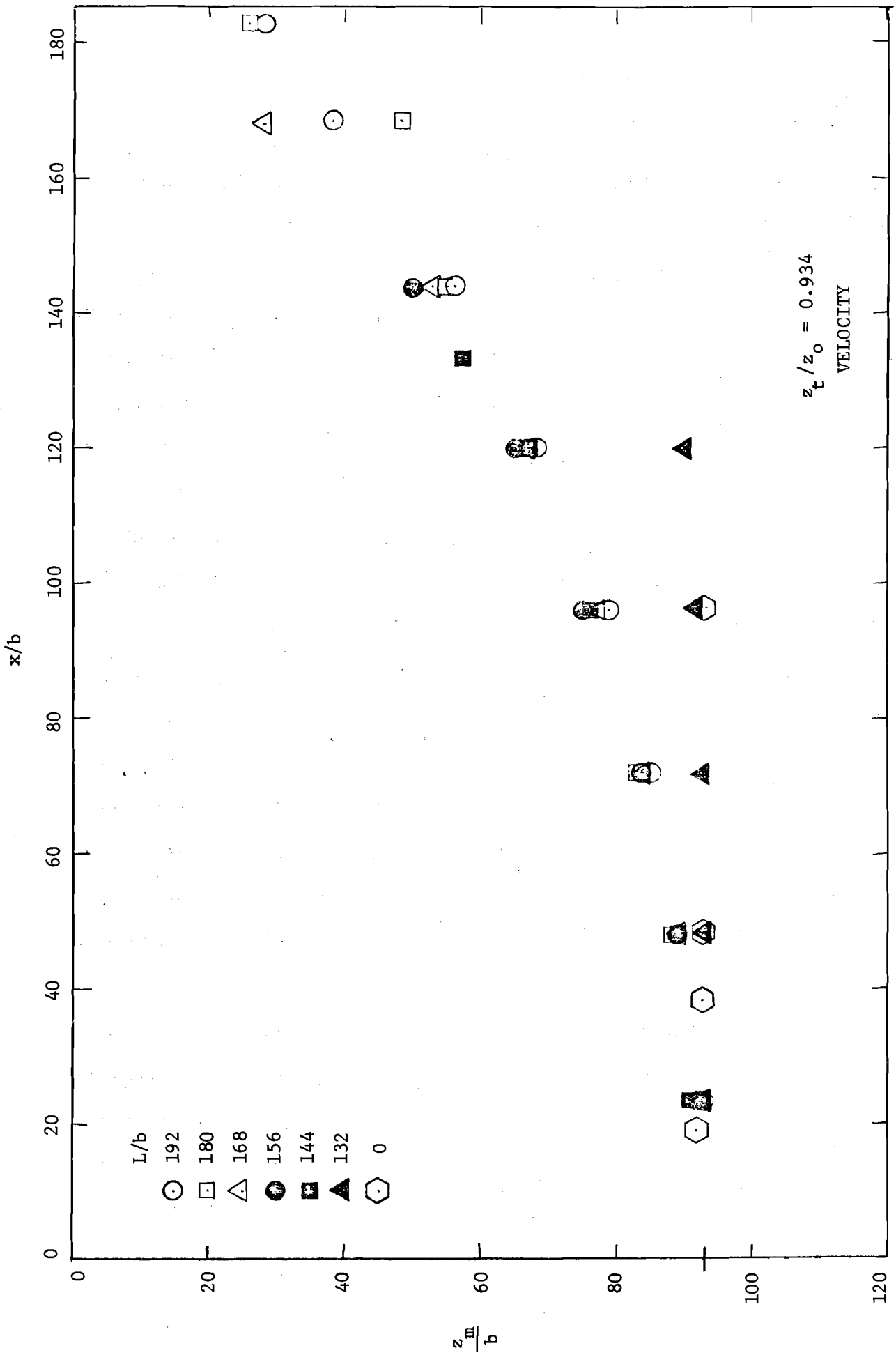

Fig. 37 Location of maximum velocity for unheated discharges between wing-walls with crests at z_t/z_o = 0.934 and slot submergence of 0.97 ft for various wing-wall lengths

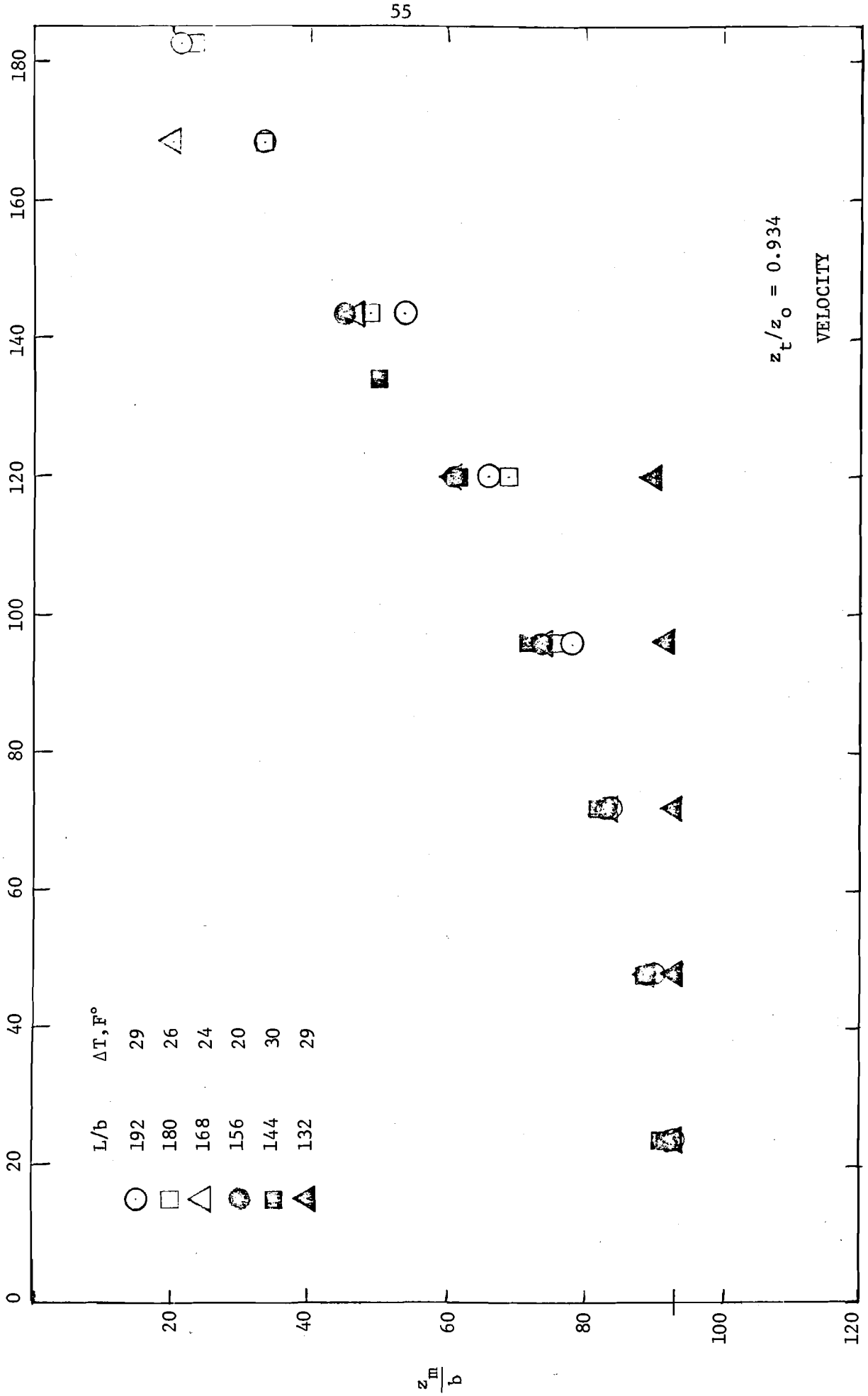

Fig. 38 Location of maximum velocity for heated discharges between wing-walls with crests at z_t/z_o = 0.934 and slot submergence of 0.97 ft for various wing-wall lengths

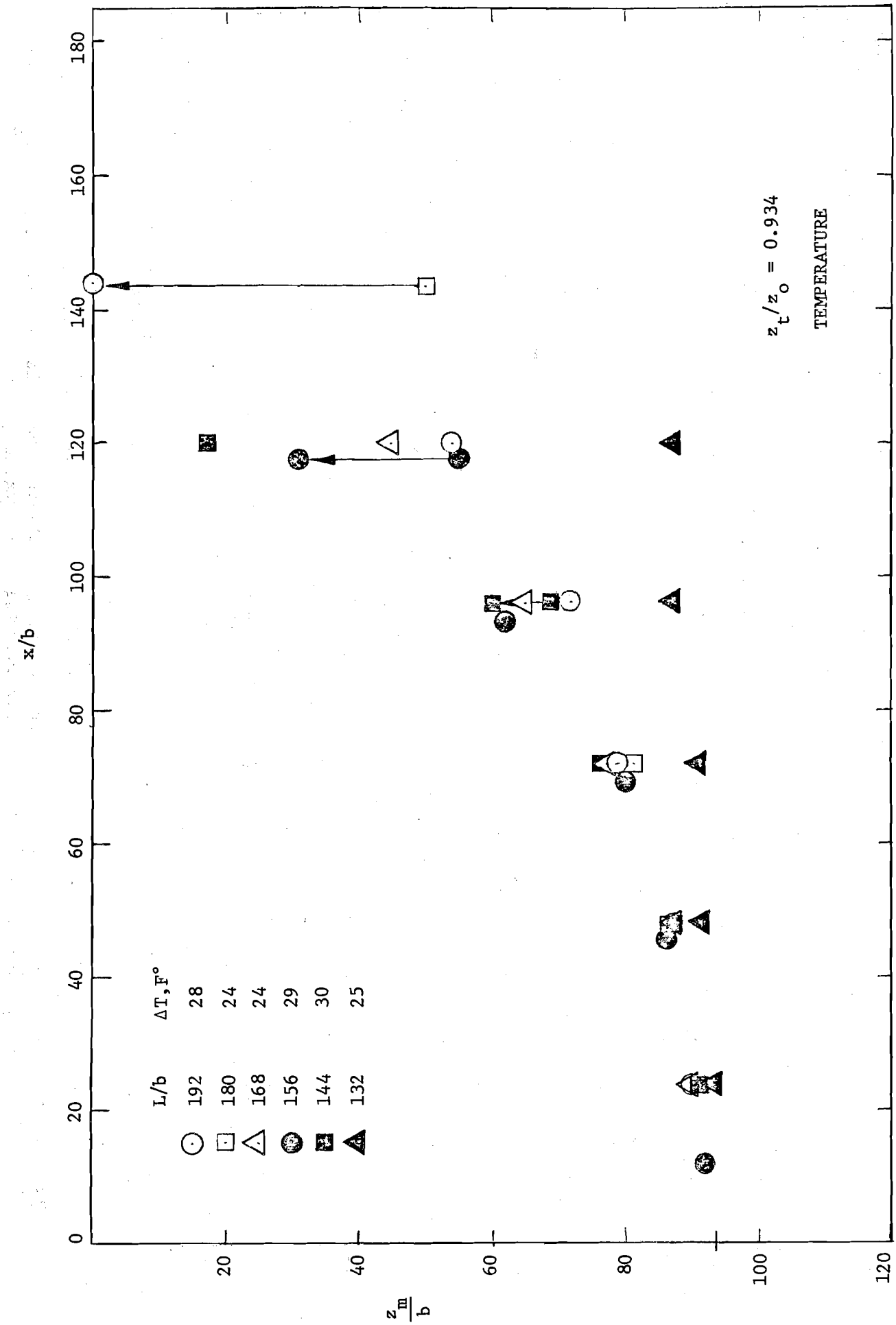

Fig. 39 Location of maximum temperature for heated discharges between wing-walls with crests at z_t/z_o = 0.934 and slot submergence of 0.97 ft for various wing-wall lengths

pattern when L/b was reduced from 144 to 132. Comparison of Figures 37 and 38 indicates very small influence of buoyancy.

Figures 40 and 41 show the unheated and heated maximum velocity traces for several wall lengths with $z_t/z_o = 1.000$. These show no evident effect of buoyancy. Moreover, control of the flow pattern is not lost as L/b is reduced from 144 to 132. This indicates that for the minimum wall length tested (L/b = 132) the flow pattern may be controlled by varying the crest of the wall from $z_t/z_o = 0.934$ to its maximum value of 1.000.

III.6 Outlet Densimetric Froude Numbers

It was indicated in Chapter II that the values of $\Delta T = T_H - T_c$ used to characterize the experiments should not be used to calculate densimetric Froude numbers since they represent conditions at the precision mixing valves rather than at the reservoir. For those experiments involving temperature traverses to determine the location of maximum temperature a record was made of the temperature at the slot outlet and also of the vertical temperature distribution outside the wing-walls and near the back wall of the reservoir. Table 6 shows a summary of some of this information. The tabulation shows the value of temperature at the outlet, T_o, as well as the temperature outside the wing-walls at elevation z_o, T_r, at various times after turning on the heaters. The time at which experimental traversing commenced and ended is also indicated. The position of the wing-wall crest and length of wing-wall is also shown. Figure 42 shows a simple correlation among the values shown in the first three columns using a least squares fit. No significant improvement was found if absolute temperatures were used, therefore the simpler version is presented. From an examination of Table 6 the increase in reservoir temperature, T_t, over T_c for a particular set of conditions may be estimated, say midway through

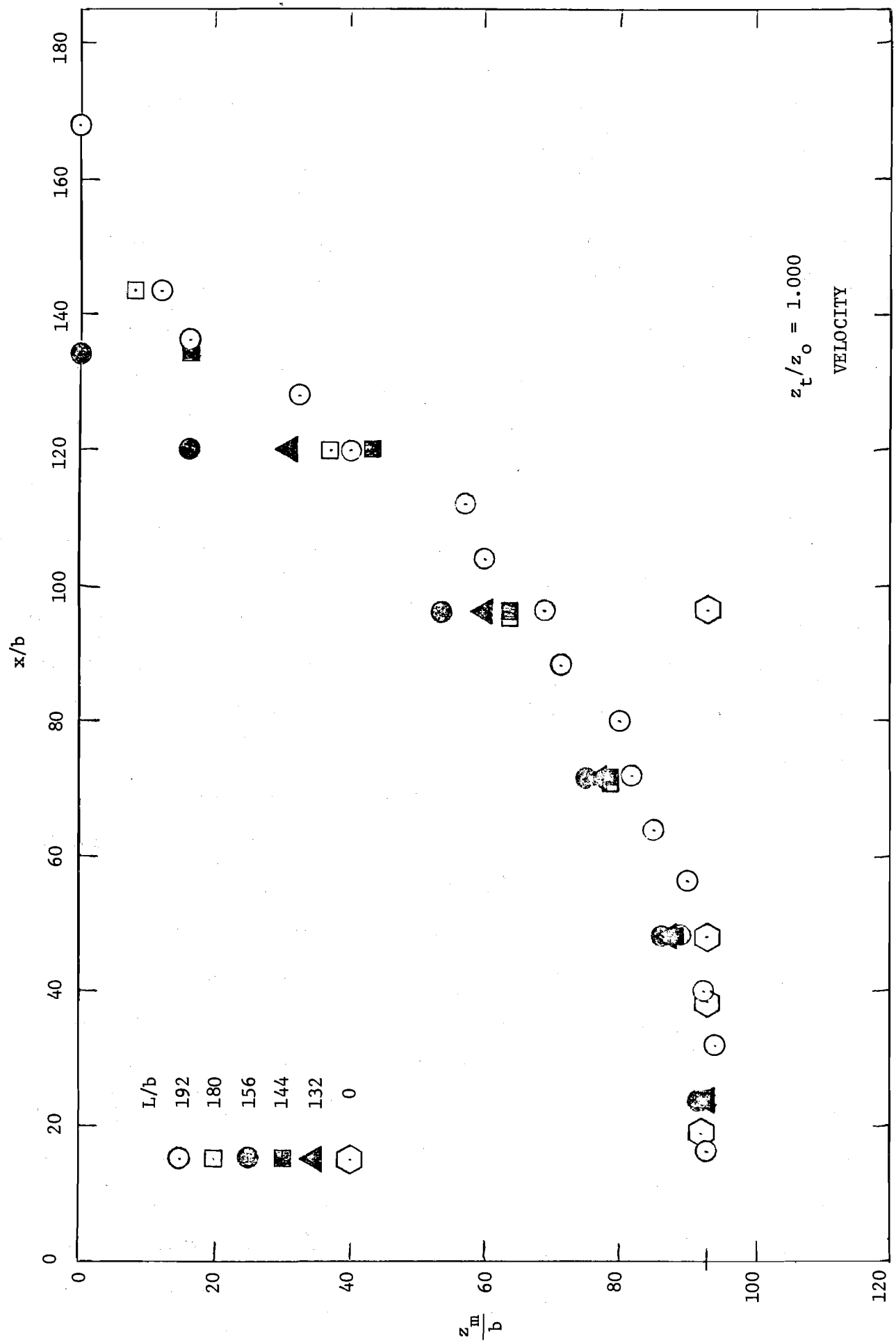

Fig. 40 Location of maximum velocity for unheated discharges between wing-walls with unsubmerged crests and slot submergence of 0.97 ft for various wing-wall lengths

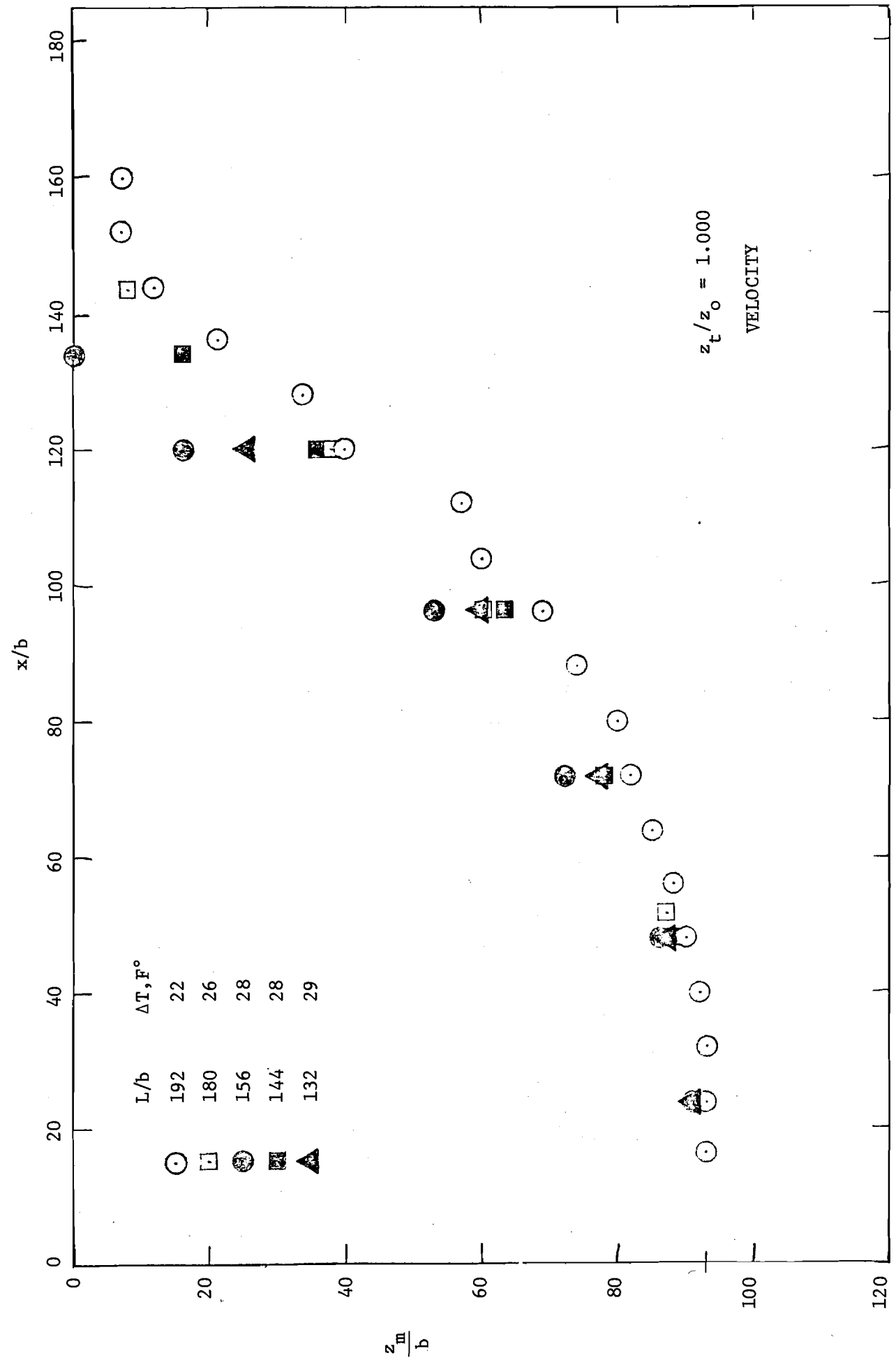

Fig. 41 Location of maximum velocity for heated discharges between wing-walls with unsubmerged crests and slot submergence of 0.97 ft for various wing-wall lengths

TABLE 6 - Summary of Temperature Conditions

T_H, °F	T_c, °F	T_o, °F	Time, mins.	T_r, °F	Exptl. progress	$\frac{z_t}{z_o}$	$\frac{L}{b}$
105	78		10	77.7		0.870	192
		97.2	30	81.1	Start		
			75	83.1	End		
			115	82.9			
105	77		30	80.4		0.956	192
		97.2	60	81.9	Start		
			140	82.4	End		
104	76		30	78.6		0.913	192
		95.5	60	80.1	Start		
			210	81.1	End		
102	74	92.5	45	76.8	Start	0.934	192
			120	78.3	End		
94	70	83.8				1.000	180
95	71	86.4	45	74.3	Start	0.934	168
			105	75.0	End		
96	67	84.2	30	70.2	Start	0.934	156
			200	72.3	End		
96	69	85.1				1.000	156
96	70	86.0	30	72.1	Start	0.934	144
			165	72.9	End		
92	67	81.9	30	67.5	Start	0.934	132
			100	67.6	End		

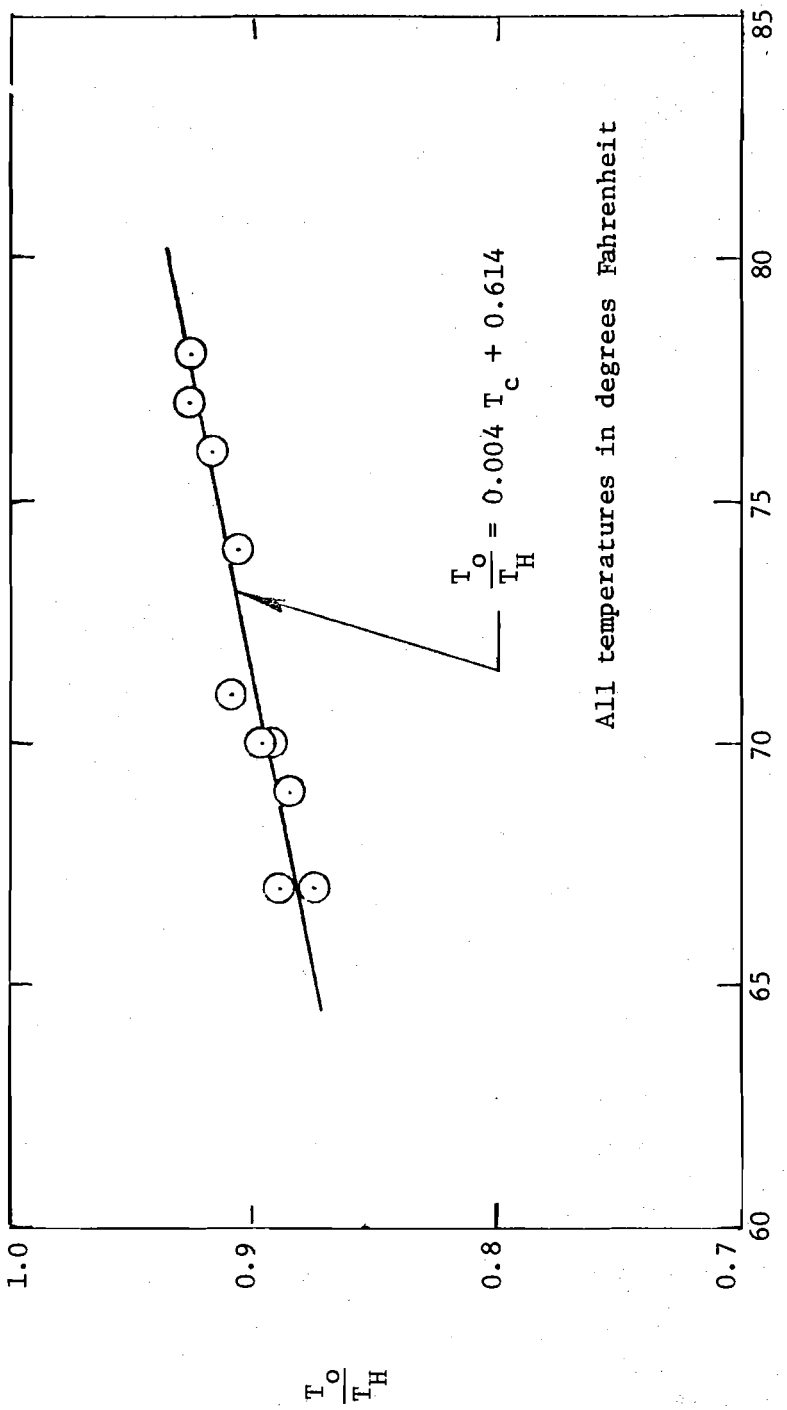

Fig. 42 Correlation between outlet temperature and mixing valve temperature

the experiment. Suppose, for example, that it is desired to calculate a characteristic densimetric Froude for one of the experiments listed in Table 4, namely for the heated velocity traverse with $z_t/z_o = 0.934$. In this case $T_H = 102°F$, and $T_c = 73°F$. From Fig. 42 $T_o = 92.4°F$. Table 6 indicates that for $z_t/z_o = 0.934$, L/b = 192 the value of T_r midway through the experiment was approximately 3.5 F° above T_c. The appropriate representative reservoir temperature in this case would then be 76.5°F. This gives $\Delta\rho/\rho = 0.002626$ and a densimetric Froude number based on the slot width, w, of magnitude $F_\Delta = u_o/(gw\Delta\rho/\rho)^{0.5} \approx 40$. This magnitude of densimetric Froude number is typical of all the experiments involving heated water.

III.7 Stability of the Flow Pattern

It was noted in Section III-2 that, after the installation of the wing-walls, it was necessary to reduce the outlet velocity from approximately 30 ft/sec to approximately 8 ft/sec in order to avoid unstable pulsating behavior with submergence of the outflow only occurring on an intermittent basis. Therefore a series of tests was conducted in which outlet velocities and submergences were varied. A single observer made a judgement, from an observation of the flow pattern, that it was stable or unstable. A stable flow pattern was one for which the outflow remained submerged at all times. It should be noted that this also resulted in quite different behavior of the velocity record at a downstream station than when the flow pulsated. In the latter circumstance the signal had a substantial cyclic component. Nevertheless, it was felt that the character of the flow could be judged by observation alone. In order to determine the appropriate length dimension to be used in a correlation of the data a 1/8-in. aluminum plate which extended from the floor of the reservoir

through the free surface and from the outlet to a distance of 22-in. downstream was installed so as to divide the flow region between the wing-walls into two symmetric parts. The experiments were repeated and the nature of the flow pattern in the reduced outlet configuration observed. It was assumed that the discharge was evenly divided by the 1/8-in. splitter plate.

The results of the observations are presented in Figure 43 in which a linear relationship is found to indicate neutral stability when the submergence expressed in wall widths is plotted against a Froude number based on average velocity at the outlet and width between the walls, w.

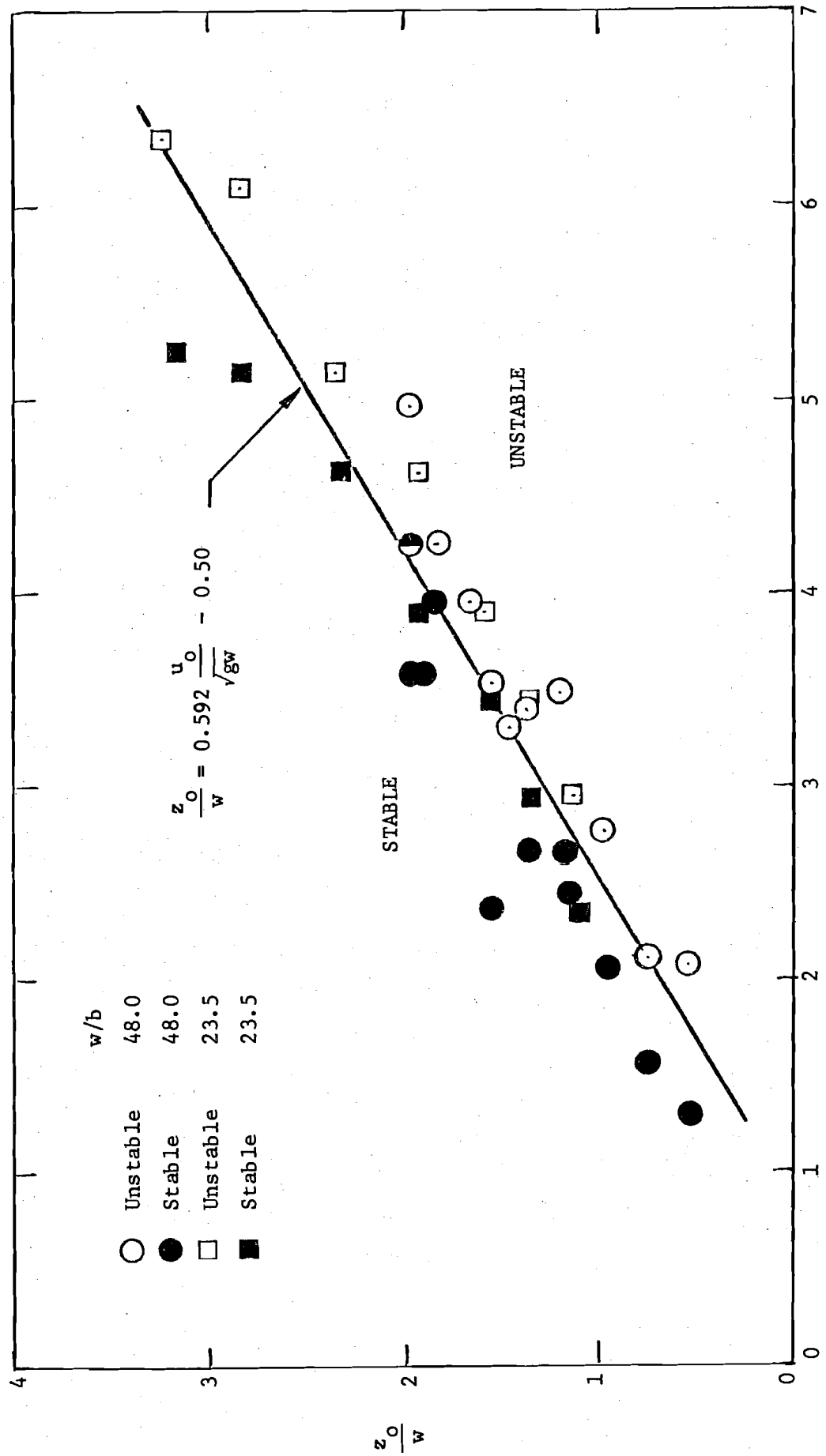

Fig. 43 Stability of the flow pattern for range of flow conditions

IV. DISCUSSION AND CONCLUSIONS

IV.1. Discussion of Test Results

Figure 37 has been reproduced as Figure 44, with the various positions of the wing-wall crest and downstream end superimposed on it. The two positions of the downstream top corner for which loss of control of the flow pattern was observed are emphasized by hatching, namely L/b = 192 for $z_t/z_o = 0.870$ and L/b = 132 for $z_t/z_o = 0.934$. The two corresponding points at which the ends of the walls intersect the filament of maximum velocity have been joined by the line labelled AA. Until further data is obtained this line or its extension may be used as a guide in estimating the length of wall at which control is lost for a particular wall crest elevation. The character of the data presented previously indicate that most decisions on the behavior of the flow pattern may be made by referring to the trace of the filament of maximum velocity for an unheated discharge. For example, there is no discernible difference in the behavior as characterized by Figs. 37, 38 and 39. Since the temperature profiles tend to be somewhat flatter than the velocity profiles the location of the maximum is more difficult. Focussing attention therefore on Figure 37 it may be noted that there was no significant change in position of the filament of maximum velocity for wall length to slot height ratios ranging from 192 down to 144 when the wall top was held at a constant position $z_t/z_o = 0.934$. Then as L/b was reduced to 132 control was suddenly lost. This suggests that the entrainment requirements on top of the jet were satisfied by water moving into the region above the filament of maximum velocity around the downstream ends of the wing-walls.

It would appear that a structure corresponding to L/b = 132 with the wall crest set at $z_t/z_o = 0.934$ would be too sensitive to wall-top gate

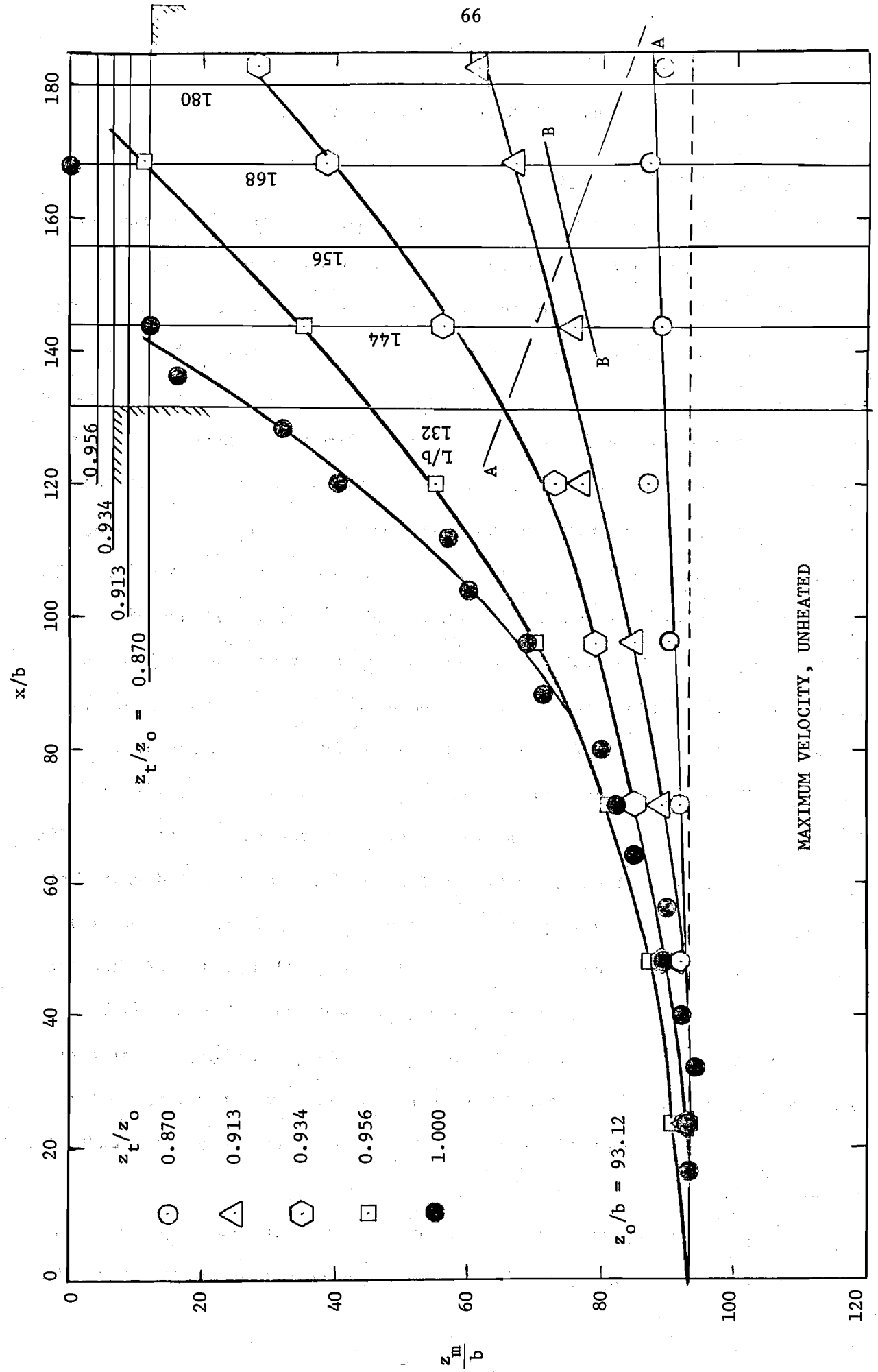

Fig. 44 Figure 40 with wall positions and loss of control line superimposed

position to permit ease of control of the flow pattern. The gate elevation could only range over 6.6 per cent of the submergence. The original condition tested, namely with L/b = 192 and the crest set at $z_t/z_o = 0.870$ allows the gate elevation to range over 13 per cent of the submergence. However the penalty for decreased sensitivity is increased wall length.

It may also be noted that the Illinois data presented in Fig. 30 for complete wing-walls may be collapsed to a single plot as shown in Fig. 45. To this graph could be added the data collected by John et al (2) and by Stoy et al (8). This suggests that for submergences other than 0.97 ft the length of the wing-walls should be determined as multiples of submergence, z_o rather than of slot height, b, with the behavior for various submergences inferred from Fig. 44.

IV.2. Suggested Design Procedure

A suggested design procedure making use of the limited data which has been collected will be illustrated using an example. Suppose that it is desired to construct a facility discharging 1000 cfs, that the design submergence of the outlet centerline is 10 ft, the outlet is to be 2 ft high and that the control gates on the crest of the wall are to range over 1 ft. The problem is to select an appropriate width of basin to have a stable flow pattern and to select a wall length that will be adequate to permit control over the 1 ft range of the gates. From Fig. 43 the neutral stability width is given by:

$$\frac{10}{w} = \frac{52.25}{w^{3/2}} - 0.50$$

for which w = 11.2 ft. This is the neutral width; therefore increase w to at least 12 ft for stability. Next, since z_t/z_o is to be 0.900 make a linear interpolation on Fig. 44 between the curves for $z_t/z_o = 0.870$

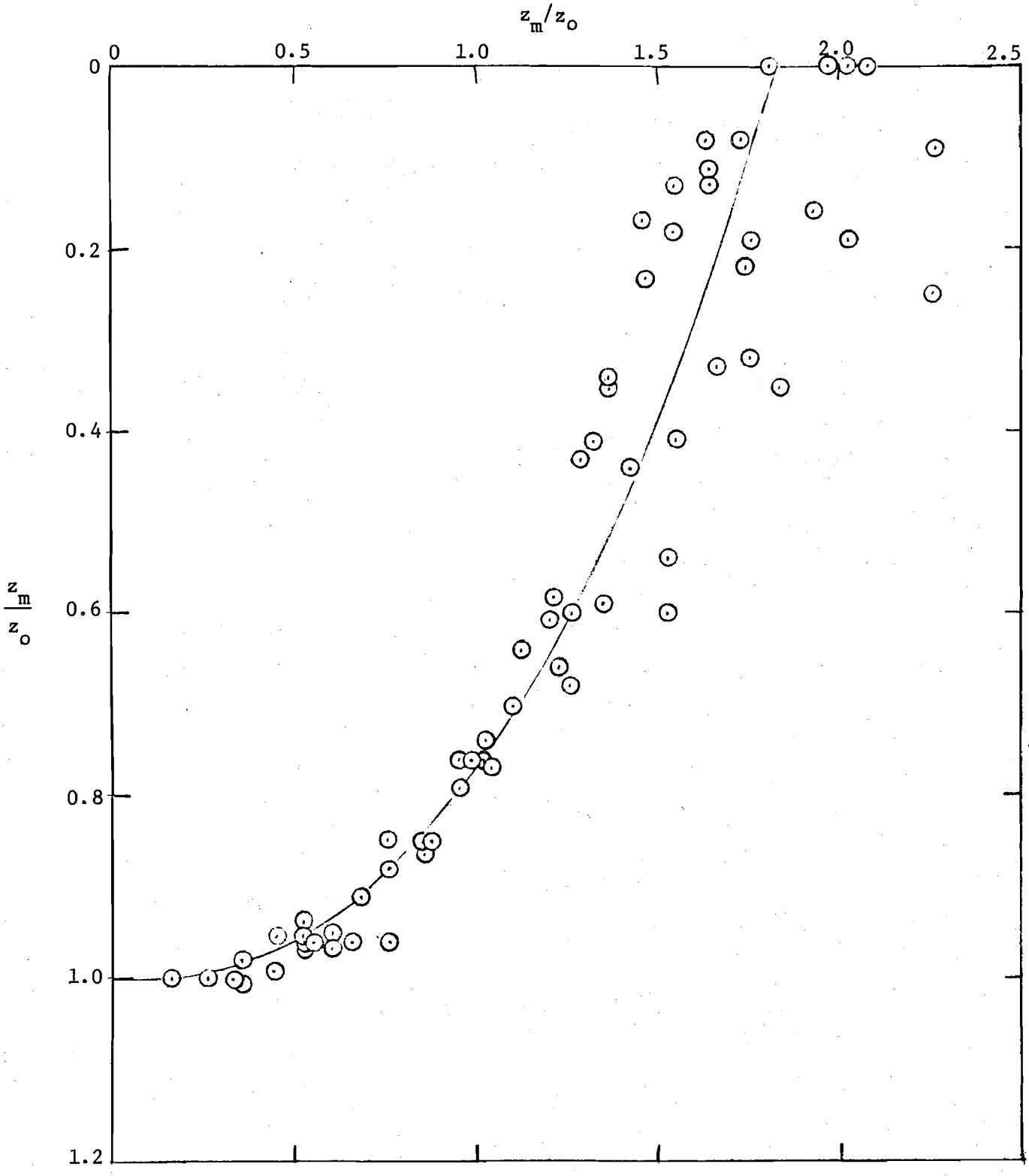

Fig. 45 Location of maximum velocity for heated and unheated discharges between complete wing-walls with L/b = 192 for several slot submergences

and 0.913. This is indicated by BB on Fig. 44. BB crosses AA at x/b = 157 for z_o/b = 93.12. Thus the end of the wall should be 157/93.12 = 1.69 slot submergences from the outlet. In this case therefore the wall length should be at least 17 feet.

IV.3. Summary and Conclusions

Detailed velocity traverses have been obtained for three different shallow submergences of a slot outlet forty-eight times as wide as it was high, for Reynolds numbers based on outlet width and exit velocity of order 1,500,000. The outlet was unconfined laterally.

Traces of the filament of maximum flux were made when wing-walls flush with the sides of the slot were added. Tests were conducted for various wing-wall crest elevations and various wing-wall lengths. Both heated and unheated effluents were tested.

A typical Reynolds number based on slot width and average velocity for these tests is of order 400,000. For the heated tests a typical densimetric Froude number based on average outlet velocity and slot width is 40.

Although velocity traverses were taken for the heated and unheated discharges and temperature traverses taken for heated discharges it was found that the behavior of the flow pattern for a particular wing-wall geometry could be adequately characterized using the velocity traverses for an unheated discharge.

The flow pattern was found to be surging and unstable for some combinations of outlet submergence and discharge rate. A series of tests were conducted to delineate the limits of stability.

In conclusion, it has been demonstrated that flow patterns may be controlled using wing-walls with control of discharge over the wing-wall crests. A simple design procedure making use of the data presented

on Figs. 43, 44 and 45 has been illustrated in Section V.4. This could be improved with the collection of additional data.

LIST OF REFERENCES

1. Albertson, M. L., Dai, Y. B., Jensen, R. A., and Rouse, H., "Diffusion of Submerged Jets," Trans. Amer. Soc. Civil Engrs., Vol. 115, 1950, pp. 639-697.

2. John, J.E.A., Mahajan, B., and Kanbour, S., "Mixing Studies Associated with Thermal Pollution," Univ. of Maryland Water Resources Research Center Completion Reports, No. A-007-MD, Dec. 1970, 77 pp.

3. Mahajan, B. M., and John, J.E.A., "Mixing of Shallow Submerged Heated Water Jet with an Ambient Reservoir," AIAA Journal, Vol. 9, No. 11, Nov. 1971, pp. 2135-2140.

4. Maxwell, W.H.C., and Pazwash, H., "Basic Study of Jet Flow Patterns Related to Stream and Reservoir Behavior," Univ. of Illinois Water Resources Research Center Reports, No. 10, July 1967, 63 pp.

5. Maxwell, W.H.C., and Pazwash, H., "Boundary Effects on Jet Flow Patterns Related to Water Quality and Pollution Problems," Univ. of Illinois Water Resources Research Center Reports, No. 28, Jan. 1970, 84 pp.

6. Maxwell, W.H.C., and Pazwash, H., "Axisymmetric Shallow Submerged Turbulent Jets," Journal of the Hydraulics Division, ASCE, Vol. 99, No. HY4, Proc. Paper 9675, April 1973, pp. 637-652.

7. Mross, J. J., "The Effect of a Free Surface upon the Velocity Distribution of a Submerged Jet," thesis presented to the University of Iowa, at Iowa City, Iowa, in Feb. 1960, in partial fulfillment of the requirements for the degree of Master of Science.

8. Stoy, R. L., Stenhouse, M. H., and Hsia, A., "Vortex Containment of Submerged Jet Discharge," Journal of the Hydraulics Division, ASCE, Vol. 99, No. HY9, Proc. Paper 9999, Sept. 1973, pp. 1585-1597.

9. Trentacoste, N., and Sforza, P. M., "An Experimental Investigation of Three-Dimensional Free Mixing in Incompressible, Turbulent, Free Jets," Polytechnic Institute of Brooklyn, PIBAL Reports, No. 871, March 1966, 66 pp.

10. Trentacoste, N., and Sforza, P., "Further Experimental Results for Three-Dimensional Free Jets," AIAA Journal, Vol. 5, No. 5, May 1967, pp. 885-891.

11. Trentacoste, N., and Sforza, P., "Some Remarks on Three-Dimensional Wakes and Jets," AIAA Journal, Vol. 6, No. 12, Dec. 1968, pp. 2454-2456.